

PKC epsilon Promotes Synaptogenesis through Membrane Accumulation of the Postsynaptic Density Protein PSD-95

Abhik Sen, Jarin Hongpaisan, Desheng Wang, Thomas J. Nelson and Daniel L. Alkon.

Blanchette Rockefeller Neurosciences Institute,
8 Medical Center Drive, Morgantown, WV 26505, USA.

Running Title: *PKCε induces synaptogenesis via PSD-95*

To whom the correspondence should be addressed: Dr. Abhik Sen, PhD, Blanchette Rockefeller Neurosciences Institute, 8 Medical Center Drive, Morgantown, WV 26505, USA.
Telephone: +1-304-293-9222; Fax: +1-304-293-7536; E-mail address: asen@brni.org

Keywords: Synapse, protein kinase C, phosphorylation, scaffold protein, protein translocation, PSD-95.

ABSTRACT

Protein kinase C epsilon (PKCε) promotes synaptic maturation and synaptogenesis via activation of synaptic growth factors such as BDNF, NGF, and IGF. However, many of the detailed mechanisms by which PKCε induces synaptogenesis are not fully understood. Accumulation of PSD-95 to the postsynaptic density (PSD) is known to lead to synaptic maturation and strengthening of excitatory synapses. Here we investigated the relationship between PKCε and PSD-95. We show that the PKCε activators DCPLA-ME and bryostatin 1 induce phosphorylation of PSD-95 at the serine-295 residue, increase the levels of PSD-95, and enhance its membrane localization. Elimination of the serine-295 residue in PSD-95 abolished PKCε-induced membrane accumulation. Knockdown of either PKCε or JNK1 prevented PKCε activator-mediated membrane accumulation of PSD-95. PKCε directly phosphorylated PSD-95 and JNK1 *in vitro*. Inhibiting PKCε, JNK, or CaMKII activity prevented the effects of PKCε activators on PSD-95 phosphorylation. Increase in membrane accumulation of PKCε and phosphorylated PSD-95 (p-PSD-95^{S295}) coincided with increased number of synapses and increased amplitudes of excitatory post-synaptic potentials (EPSPs) in adult rat hippocampal slices. Knockdown of PKCε also reduced the synthesis of PSD-95 and the presynaptic protein synaptophysin by 30% and 44% respectively. Prolonged activation of PKCε increased synapse number by 2-fold, increased presynaptic vesicle density, and

greatly increased PSD-95 clustering. These results indicate that PKCε promotes synaptogenesis by activating PSD-95 phosphorylation directly, through JNK1 and CaMKII, and also by inducing expression of PSD-95 and synaptophysin.

Protein kinase C epsilon (PKCε) is one of the novel PKC isotypes and is characterized as a calcium independent and phorbol ester/diacylglycerol-sensitive serine/threonine kinase. Among the novel PKCs, PKCε is the most abundant species in the central nervous system, mediating various neuronal functions (1-2). In neuroblastoma cells overexpression of PKCε, but not PKCα, βII or δ leads to neurite outgrowth through interaction of actin filaments and the C1 domain of PKCε (3-5). The actin binding site of PKCε is also implicated in exocytosis of neurotransmitters (6). PKCε is essential for many types of learning and memory (7-8) and neuroprotection (9-13). Neuronal contact with astrocytes also promotes global synaptogenesis through PKCε signaling (14). PKCε activation has been shown to promote the maturation of dendritic synapses during associative learning (9). PKCε activation also protects against neurodegeneration (10,15). Phosphorylation of long-tailed AMPARs GluA4 and GluA1 by PKC promotes their surface expression (16-17). PKC activation induces protein synthesis required for long-term memory (12,18). PKCε activation is also required for HuD-mediated mRNA stabilization of neurotrophic factors (19) and ApoE mediated epigenetic

regulation of BDNF (20). PKC activation induces translocation of calcium/calmodulin-dependent kinase II (CaMKII) to synapses (21) where it participates in PSD-95-induced synaptic strengthening (22). PKC also promotes NMDA receptor trafficking by indirectly triggering CaMKII autophosphorylation and subsequent increased association with NMDARs (23).

Thus, a number of studies have suggested that PKC activators such as bryostatin and dicyclopropanated linoleic acid methyl ester (DCPLA-ME) may be useful therapeutic candidates for the treatment of Alzheimer's disease (AD) and other causes of synaptic loss such as ischemia, stroke, and Fragile X syndrome (5-6,14,24). Some of these benefits have been attributed to induction of neurotrophic factors such as BDNF or the activation of anti-A β repair pathways and anti-apoptotic activity (10,13,20,25). However, the biochemical mechanisms by which PKC ϵ induces synaptogenesis and mediates neuroprotection are still not fully understood.

At excitatory synapses, the postsynaptic density is characterized by an electron-dense thick matrix that contains key molecules involved in the regulation of glutamate receptor targeting and trafficking (26). PSD-95 is an abundant scaffold protein in excitatory synapses, where it functions to cluster proteins such as glutamate receptors on the postsynaptic membrane and couples them to downstream signaling molecules, thereby inducing the surface expression and synaptic insertion of glutamate receptors (27-29). In addition to its role in synaptic function, PSD-95 has also been proposed to affect synapse maturation and stabilization (30-32) and thus, synapse number. Phosphorylation of the serine-295 residue of PSD-95 enhances the synaptic accumulation of PSD-95 and its ability to recruit surface α -amino-3-hydroxy-5-methyl-4-isoxazolepropionic acid (AMPA) receptors and potentiate excitatory postsynaptic currents (33).

In the present study, we examined the role of PKC ϵ signaling and PKC ϵ activators in PSD-95 regulation and induction of synaptogenesis in cultured neurons and CA1 hippocampal slices. We report that PKC ϵ activation induces membrane translocation and phosphorylation of PSD-95 at the serine-295 residue, coinciding with an increased number of synapses. Our data suggest that an important mechanism by which PKC ϵ

induces synaptogenesis is by increasing the phosphorylation of PSD-95 at the postsynaptic site and by regulating the expression of synaptophysin at the presynaptic site.

RESULTS

PKC activation prevents degradation of primary human neurons- PKC ϵ is present in high concentration in central neuronal tissues and has been implicated in broad spectrum neuronal functions. To determine the effect of PKC ϵ activation on survival and maintenance, primary human neurons were treated for 40 days with two different PKC activators (bryostatin 1 and DCPLA-ME, which are relatively specific for PKC ϵ) (13,34-36). Culture media and activators were changed every three days. Cells were imaged from three independent wells every five days and neurite positive cells were counted from 508 μ m² field images. Cells treated with either DCPLA-ME (100nM) or bryostatin 1 (0.27nM) showed an improved survival with increased neuritic branching (**Fig. 1A**). Untreated cells showed degeneration and 50% cell loss by 36 days, while the treated cells remained healthy for at least 40 days (**Fig. 1B**). The number of viable neurite-positive cells was also significantly higher at 40 days ($F_{(2, 6)}=705.4$; ANOVA, $P<0.0001$) in the activator treated cells than untreated cells (bryostatin 1: 369.7 ± 12.2 ; DCPLA-ME: 334.7 ± 1.8 ; untreated 109.7 ± 6.4).

Prolonged PKC ϵ activation prevents loss of synaptic proteins- We quantified the mRNA expression of PKC ϵ , PSD-95 and synaptophysin at 40 days in untreated and PKC ϵ activator-treated neurons. At 40 days the mRNA levels of PKC ϵ ($F_{(3,8)} = 18.3$; $P=0.0006$) and PSD-95 ($F_{(3,8)} = 44.6$; $P<0.0001$) were significantly higher in the PKC ϵ activator-treated cells compared to 40 day control cells (**Fig. 1C, D**). Synaptophysin mRNA showed no significant change in between treated and untreated groups (**Fig. 1E**). We also quantified the protein expression of phosphorylated PSD-95 (p-PSD-95^{S295}), PSD-95 and synaptophysin at 40 days in untreated and PKC ϵ activator-treated neurons by immunoblot (**Fig. 1F**). Expression levels of PKC ϵ ($F_{(3,8)} = 16.60$; $P<0.001$), p-PSD-95^{S295} ($F_{(3,8)} = 66.83$; $P<0.0001$), PSD-95 ($F_{(3,8)} = 21.22$; $P<0.001$) and synaptophysin were significantly higher in the 40 day PKC ϵ activator-treated cells compared to 40 day control cells (**Fig.**

1G-J). Moreover, protein expression levels of PKC ϵ , PSD-95 and synaptophysin showed a marked decrease in 40-day untreated cells compared to 1-day cells, even after correction for total protein, while PKC ϵ activation prevented the time-dependent loss. This indicates an essential role of PKC ϵ in maintenance of synapses and preserving normal levels of both PSD-95 and synaptophysin.

Bryostatin 1 and DCPLA-ME specifically activate PKC ϵ . We then investigated whether this phenomenon is specific to PKC ϵ or whether other PKC isozymes are involved. PKC translocation to the plasma membrane generally has been considered the hallmark of activation and frequently has been used as a surrogate measure of PKC isoform activation in cells (37). Expression levels of PKC α , PKC ϵ and PKC δ in the soluble (cytosol) and particulate (membrane) were measured by immunoblot at 1hr, 4hr and 24hr after either bryostatin 1 (0.27 nM) or DCPLA-ME (100 nM) treatment (**Fig. 2A, C**). Both DCPLA-ME and bryostatin 1 increased membrane translocation of PKC ϵ but not PKC α or PKC δ (**Fig. 2B,D**), confirming that both the compounds activate PKC ϵ but not PKC α or PKC δ .

PKC ϵ activation induces membrane translocation of phosphorylated PSD-95 (serine 295). Phosphorylation of PSD-95 on Serine-295 is known to promote localization of PSD-95 in the postsynaptic density (PSD), strengthening the excitatory synapse (33). To determine whether time-dependent PKC ϵ activation has an effect on localization and expression of p-PSD-95^{S295}, we measured the expression of p-PSD-95^{S295} in the soluble and particulate fractions of the primary human neurons at 1hr, 4hr and 24hr post PKC activator treatment (**Fig. 2E, F**). PKC ϵ activation increased the level of p-PSD-95^{S295} in the particulate fraction of both bryostatin 1 ($F_{(3,8)}=4.9$; ANOVA, $P=0.03$) and DCPLA-ME treated cells ($F_{(3,8)}=11.7$; ANOVA, $P=0.003$) (**Fig. 2F**). The total PSD-95 expression in whole cell lysate from primary human neurons was unchanged among different groups (**Fig. 2E**). At 4hr p-PSD-95^{S295} levels were significantly higher in bryostatin 1 (156.4 ± 14.9 %; $P=0.01$) and DCPLA-ME (160.1 ± 9.5 %; $P=0.003$) treated neurons compared to untreated neurons. In adult rat hippocampal slices PKC ϵ activation increased p-PSD-95^{S295} expression at 1hr and 4hr (bryostatin 1: $F_{(3,8)}$

$=4.95$; ANOVA $P=0.031$ and DCPLA-ME: $F_{(3,8)}=4.34$; ANOVA $P=0.043$). (**Fig. 2G, H**). Negligible amounts of p-PSD-95^{S295} were detected in the soluble fraction. These results show that the increase in membrane localization of p-PSD-95^{S295} corresponded with the kinetics of PKC ϵ activation at 1hr and 4hr.

PKC ϵ -mediated phosphorylation of PSD-95 at serine-295 is essential for its membrane association- Purified recombinant human PSD-95 (r-PSD-95) protein was readily phosphorylated by activated recombinant PKC ϵ (r-PKC ϵ) *in vitro*, and the PKC inhibitor bisindolylmaleimide I (Go 6850) (BisI: 100nM) blocked the reaction (**Fig. 3A**). Both bryostatin 1 and DCPLA-ME increased the amount of p-PSD-95^{S295} *in vitro* compared to unactivated PKC alone (Bryostatin 1 + r-PKC ϵ + r-PSD-95: 200.3 ± 5.06 %, $P=0.004$; DCPLA-ME + r-PKC ϵ + r-PSD-95: 194.6 ± 12.95 %, $P=0.032$; r-PKC ϵ + r-PSD-95 control: 146.9 ± 7.06 %) (**Fig. 3B**). The PKC inhibitor BisI blocked the phosphorylation. These results show that PKC ϵ can phosphorylate PSD-95 at serine 295 *in vitro*.

Next we tested if the serine-295 residue in PSD-95 is essential for its membrane translocation. We created two separate clones, one containing the wild type human PSD-95, and the other containing mutant-PSD-95^{S295K}, in which the serine residue at 295 (AGT) was changed to lysine (AAA). Both the clones were transfected and expressed in HEK-293 cells and their expression was measured by immunoblot. Both transfected cell lines showed PSD-95 immunoreactivity against a PSD-95 antibody raised against the N-terminal region of PSD-95. The anti-p-PSD-95^{S295} antibody showed positive bands only with the wild type PSD-95 transfected cell lysate. Untransfected HEK-293 cells showed no PSD-95 expression (**Fig. 3C**). The wild PSD-95 and PSD-95^{S295K} expressing HEK-293 cells were then treated with bryostatin 1 and DCPLA-ME for 4hr in presence or absence of PKC ϵ translocation inhibitor (EAVSLKPT; 5 μ M) and fractionated into cytosol and membrane fractions. Only small amounts of p-PSD-95 were found in soluble fractions (**Fig. 3D**). As expected, bryostatin 1 and DCPLA-ME significantly increased membrane translocation of PKC ϵ in both PSD-95 and PSD-95^{S295K} expressing cells (in wild-type cells: bryostatin 1 = 54.4 ± 4.9 %, $P=0.0004$ and DCPLA-ME = 19.1 ± 4.2 %, $P=0.01$; $F_{(4,10)}=28.8$, ANOVA $P<0.0001$) (**Fig.**

3E). PKCε activators also increased translocation of wild-type PSD-95 (bryostatin 1: $+ 29.9 \pm 2.3\%$, $P=0.0002$; DCPLA-ME: $+ 20.5 \pm 2.5\%$, $P=0.001$; $F_{(4,10)}=35$, ANOVA $P<0.0001$), but not mutated PSD-95^{S295K}, which lacks the PKCε phosphorylation site ($F_{(2,6)}=0.75$, ANOVA $P=0.51$) (**Fig. 3F**).

To further verify that phosphorylation at serine-295 is essential for membrane association, we immunoblotted the membrane fraction against anti-p-PSD-95^{S295} antibody. The level of p-PSD-95^{S295} in the membrane was increased in the PKCε activator treated cells (bryostatin 1: $151.7 \pm 6.1\%$, $P=0.002$ and DCPLA-ME: $161.1 \pm 10.4\%$, $P=0.004$ ($100 \pm 2.8\%$); $F_{(4,10)}=27.4$, ANOVA $P<0.0001$) (**Fig. 3G**). Membrane p-PSD-95^{S295} translocation was blocked by the PKC inhibitor. Together, these results indicate that PKCε activation phosphorylates the serine-295 residue of PSD-95 and this phosphorylation is necessary for membrane accumulation of PSD-95.

PKCε-mediated membrane localization of p-PSD-95^{S295} involves JNK1 and CaMKII

Previously it has been reported that accumulation of PSD-95 in the PSD is increased by synaptic activity and by a Rac1-JNK1 signaling pathway (33). PKCε is involved in JNK activation in macrophages (38-39) and CaMKII inhibitors inhibit PKC-mediated signaling in hippocampal neurons (40). Thus we investigated the involvement of PKCε, JNK and CaMKII in PSD-95^{S295} translocation in primary human neurons. Cells were pretreated for 30 min with BisI (Go 6850) (100 nM, PKC inhibitor), SP600125 (20μM, JNK inhibitor) or KN-93 (10μM, CaMKII inhibitor) and then treated with PKCε activators for 4hr. Cells were fractionated into cytosolic and membrane fractions and the membrane fractions were analyzed for the expression of p-PSD-95^{S295}. The inhibitors alone reduced the expression of membrane bound p-PSD-95^{S295} ($F_{(4,10)}=23.04$; ANOVA $P<0.0001$) (**Fig. 4A,C**). DCPLA-ME treatment increased membrane localization of p-PSD-95^{S295} ($147.3 \pm 2.8\%$; $F_{(5,12)}=39.2$; ANOVA $P<0.0001$). PSD-95 phosphorylation was prevented by blocking PKC activation using bisindolylmaleimide I (**Fig. 4B,D**), confirming the involvement of PKCε in localization of p-PSD-95^{S295} in the membrane. The JNK inhibitor SP600125 and the CaMKII inhibitor K-93 also

prevented PKCε-mediated phosphorylation and translocation of PSD-95 (**Fig. 4B,D**).

PKCε phosphorylated PSD-95 *in vitro*, incorporating 1.46 ± 0.05 moles of ³²P-ATP per mole of PSD-95. Western blotting with p-PSD-95^{S295}-specific antibody confirmed that this included the Ser-295 site (**Fig. 3A,B**). PKC and JNK inhibitors fully inhibited the PKCε mediated PSD-95 phosphorylation, while a CaMKII inhibitor partially prevented PSD-95 phosphorylation (**Fig. 4E**). PKCε also phosphorylated JNK1 *in vitro*, incorporating 1.02 ± 0.04 moles of ³²P-ATP per mole of JNK1; BisI prevented JNK1 phosphorylation (**Fig. 4F**). PKC is also reported to phosphorylate CaMKII *in vitro* (41), we also found increase in phosphorylation of CaMKII by PKCε (**Fig. 4G**). Since both JNK and CaMKII inhibitors prevented PSD-95 phosphorylation by PKCε (**Fig. 4E**), we considered the possibility that the JNK inhibitor might not be specific. Therefore we performed a siRNA knockdown of PKCε and JNK in human neurons. PKCε or JNK knockdown caused a 50% reduction in their respective protein expression (**Fig. 4H**). DCPLA-ME failed to induce the membrane accumulation of p-PSD-95^{S295} in PKCε and JNK knockdown human neurons ($F_{(5,12)}=24.6$; ANOVA $P<0.0001$) (**Fig. 4I,J**). These results confirm that PKCε is required for membrane translocation of p-PSD-95^{S295} and that JNK and CaMKII are intermediates in the pathway (**Fig. 4K**).

PKCε activation induces synaptogenesis in adult hippocampal slices- Next we investigated if PKCε mediated phosphorylation of PSD-95 at serine-295 leads to synaptogenesis. Since 4hr PKCε activator treatment produced the highest p-PSD-95^{S295} level, we quantified the number of synapses from within 100 μm² of 30–35 CA1 regions from untreated, bryostatin 1 and DCPLA-ME treated slices using electron microscopy (3 different slices in each group) (**Fig. 5A**). Both bryostatin 1 and DCPLA-ME increased the number of synapses at 4hr compared to only vehicle treated control (8.97 ± 0.63 , $P=0.002$, $n=35$, 6.97 ± 0.50 , $P=0.04$; $n=30$, and 5.77 ± 0.50 ; $n=35$ CA1 areas, respectively) (**Fig. 5B**). Presynaptic vesicle density was measured in a series of 3D stacked images from 6–10 presynaptic boutons from 3 different hippocampal slices. Bryostatin 1 treatment increased

presynaptic vesicle density at 4hr (93.23 ± 4.1 , $P < 0.001$, $n=30$ presynaptic boutons) in comparison to control (71.33 ± 4.45 , $n=22$ presynaptic boutons).

Next we investigated the effect of bryostatin 1 on basal synaptic transmission of hippocampal CA1 pyramidal neurons to determine whether the new synapses are functional. Field potential recordings were measured from rat hippocampal slices. An input-output curve was calculated with stimulus intensity versus the slope of EPSPs elicited in response to increasing intensity of stimulation to the Schaffer collateral. The mean EPSP slope increased with stronger intensity of stimulus. Slices preincubated with bryostatin 1 for 1hr exhibited greater EPSP slope without any change in fiber volley amplitude. This was abolished with 30 min pretreatment with the PKC inhibitor bisindolylmaleimide I (Go 6850) (BisI: 100nM) (**Fig. 5C, D**). Bryostatin 1 increased the area under the curve, which represents the overall basal synaptic transmission, and a PKC inhibitor prevented the increase (bryostatin1: 0.71 ± 0.08 , $P=0.03$; BisI+bryostatin 1: 0.49 ± 0.07 and untreated (ethanol only): 0.51 ± 0.06) (**Fig. 5E**). Treatment of slices for 4hr with bryostatin (12 slices, 3 rats) dramatically increased the EPSP slope compared to the ethanol-treated slices (6 slices, 3 rats) (**Fig. 5F,G**). The smaller response in the 4hr untreated slices compared to 1hr untreated slices may be attributed to the vehicle (ethanol) added to the slices. EPSPs in hippocampal slices are reduced by a smaller percentage after ethanol treatment (42). Thus, the prolonged treatment of slices with ethanol for 4hr may have slightly reduced the EPSP slope in these groups. Bryostatin increased the area under the curve by nearly 2 fold ($P < 0.0001$, **Fig. 5H**). These results suggest that bryostatin 1 treatment facilitates basal synaptic transmission in the Schaffer collateral commissural pathway of rat hippocampus and that the increase in EPSP slope is independent of the fiber volley.

Our results indicate that increased phosphorylation of PSD-95 by PKC ϵ leads to an increase in synapse number with increased synaptic activity. Together these data demonstrate that the new synapses are functional.

PKC ϵ knockdown reduces the expression of PSD-95 and synaptophysin- PKC ϵ is known to perform important functions both in presynaptic

(14) and postsynaptic sites. To investigate whether PKC ϵ is essential for the expression of synaptic proteins, we measured the effect of PKC ϵ knockdown (PKC ϵ KD) and PKC ϵ overexpression (PKC ϵ OE) on the expression of postsynaptic PSD-95 and presynaptic synaptophysin. Knockdown of PKC ϵ was achieved by transfecting the neurons with a mixture of siRNA containing a pool of three to five siRNAs. PKC ϵ siRNA effectively reduced PKC ϵ expression both at the mRNA and protein levels by 2- and 3.4-fold (**Fig. 6A,I**) after 72 hr. Scrambled siRNA did not cause any change in PKC ϵ expression (**Fig. 6F,G**). PKC ϵ overexpression in the neurons was obtained by transfecting pCMV6-ENTRY vector containing human PKC ϵ cDNA. Transfected neurons showed a ~ 7.4 fold increase in PKC ϵ mRNA level (**Fig. 6A**) and 3.6 fold increase in PKC ϵ protein level (**Fig. 6H, I**). Overexpressing PKC ϵ by 7-fold increased the level of synaptophysin mRNA by 59.3 ± 1.3 % and also increased the level of PSD-95 by 71.6 ± 3.8 %. Knockdown of PKC ϵ had opposite effects (**Fig. 6B, C**). PKC ϵ overexpression or knockdown did not alter SNAP-25 and syntaxin-1 mRNA levels (**Fig. 6D, E**). Loss of PKC ϵ expression reduced the protein levels of PSD-95 by 30% (0.71 ± 0.07 ; $P=0.043$) (**Fig. 6K**) and synaptophysin by 44% (0.56 ± 0.08 ; $P=0.021$) (**Fig. 6J**) compared to controls transfected with scrambled siRNA. PKC ϵ OE produced a 50% increase in synaptophysin (1.51 ± 0.1 vs 1.0 ± 0.1 in control; $P=0.015$) (**Fig. 6J**) and a 30% increase in PSD-95 expression (1.31 ± 0.08 vs 1.0 ± 0.07 in control; $P=0.024$) compared to vector-only transfected cells (**Fig. 6K**).

Knockdown of PKC ϵ reduces synaptogenesis- To further establish the role of PKC ϵ in synaptogenesis and its underlying role in expression of PSD-95 and synaptophysin we used confocal microscopy to measure the effect of PKC ϵ knockdown on the localization of PSD-95 and colocalization of PSD-95 and synaptophysin. Punctate colocalization (clusters of proximal pre- and post-synaptic markers on neurites) of PSD-95 and synaptophysin is widely accepted as an indicator of synapses (43-44). Primary human neurons were treated with bryostatin 1 or DCPLA-ME alone or after PKC ϵ KD for 10 days. PSD-95 clusters and colocalized PSD-95 and synaptophysin (as recognized by staining grains along a 40 μ m length of neurite, $n=10$) were

counted in 4 independent experiments (**Fig. 7A**). In normal cells, PKC ϵ activation by bryostatin 1 and DCPLA-ME significantly induced PSD-95 clustering in the neurites compared to untreated controls ($P < 0.05$) (**Fig. 7B**). The number of synapses was also significantly higher in cells treated with bryostatin 1 and DCPLA-ME than in untreated neurons at 10 days (**Fig. 7C**). The increase in number of synapses was independent of the neuron density. We found no change in neuron density (measured by NeuN staining) after 10 days of PKC ϵ activator treatment (**Supplementary Fig.1**). In PKC ϵ KD cells, immunofluorescence staining of human neurons showed a loss of synaptic networks, and bryostatin 1 and DCPLA-ME had no effect. PKC ϵ KD prevented the effect of PKC ϵ activators and, more importantly, reduced the basal level of PSD-95 clusters and synapses by 50%. (**Fig. 7A-C**)

We also quantified the expression levels of PKC ϵ , p-PSD-95^{S295}, PSD-95 and synaptophysin by immunoblot after 10 days of PKC ϵ -siRNA transfection (**Fig. 7D**). PKC ϵ KD cells expressed significantly lower amounts of PSD-95 ($F_{(5, 12)} = 19.24$, ANOVA $P < 0.0001$) (**Fig. 7E, F**), and synaptophysin ($F_{(5, 12)} = 12.79$, ANOVA $P = 0.0002$) (**Fig. 7G**). Bryostatin 1 and DCPLA-ME failed to induce PSD-95 and synaptophysin expression in PKC ϵ KD neurons. Bryostatin 1, but not DCPLA-ME, produced a 40% decrease in PKC ϵ protein staining (**Fig. 7D**). No loss in PKC ϵ mRNA was found in bryostatin 1-treated neurons (data not shown). Downregulation of PKC following activation by bryostatin 1 is a well documented phenomenon (45-46).

We further confirmed the effect of long term PKC ϵ activation on synaptogenesis using rat hippocampal brain slices. Slices were treated with bryostatin 1 and DCPLA-ME for 10 days. The serum-free culture medium was changed every 3 days with fresh addition of activators. Synapse number in each case was quantified using electron microscopy (**Fig. 8A**). Bryostatin 1 (7.97 ± 0.68 ; $P = 0.013$, $n = 29$ CA1 areas) and DCPLA-ME (8.71 ± 0.78 ; $P = 0.001$, $n = 24$ CA1 areas) treatment increased the number of synapses in hippocampal slices compared to vehicle-only treated slices (4.5 ± 0.45 ; $n = 24$ CA1 area) (**Fig. 8B**). Presynaptic vesicle density was also significantly higher in the bryostatin 1 (59.6 ± 6.4 , $P < 0.05$, $n = 19$ presynaptic

boutons) and DCPLA-ME (60.4 ± 5.1 , $P = 0.04$, $n = 19$ presynaptic boutons) treated slices than vehicle treated controls (48.4 ± 4.3 , $n = 20$ presynaptic boutons) (**Fig. 8C, D**). Together, these findings confirm that PKC ϵ is essential for bryostatin 1 and DCPLA-ME-mediated increase in PSD-95 and synaptophysin expression leading to increased synaptogenesis at 10 days.

DISCUSSION

The outgrowth of neurites and formation of synapses depend on interactions among a number of regulatory proteins. These interactions are required for synaptic structure rearrangement, spinogenesis, and synaptogenesis. PKC ϵ is one of the key regulators of synaptogenesis (3,24) and PKC ϵ activators promote the maturation of dendritic spines (9,47). PSD-95 is a scaffold protein which also plays an important role in formation of excitatory synapses (48-49).

Here we showed that PKC ϵ activation induces translocation and phosphorylation of PSD-95 at serine-295 residue leading to PSD-95 accumulation at the postsynaptic density. Our findings showed that PKC ϵ activation not only increased the survival of neurons but also preserved the neuronal structure. Untreated cells showed gradual degeneration over 25 days, suggesting that PKC ϵ activation is beneficial for both maturation and survival of neurons, confirming a previous report by Hama *et al.* (14). We have shown that short term acute changes in PKC ϵ activity induce structural and biochemical changes in post-synaptic density scaffolding protein PSD-95 as well as increased synaptic activity. Synaptic activity is important for neuronal survival. Synaptic activity induces expression of survival genes and suppresses pro-death genes (50). Therefore, the increased survival of neurons treated with PKC ϵ activators may be due to the increased connectivity induced in the early stages; however, other factors such as elevated neurotrophins may also play a role. PKC ϵ induces BDNF (10,19) and elevated expression and release of BDNF is associated with elevated synaptic activity, which contributes to neuroprotection (51-52).

PKC ϵ activation and membrane translocation occur both presynaptically (14,53) and postsynaptically (8) where it phosphorylates important substrate proteins required for synaptic

facilitation and synaptogenesis. We found that p-PSD-95^{S295} accumulation increased in the membrane of PKC ϵ -activated neurons and followed the same time course as PKC ϵ activation at 1hr and 4hr. The serine-295 residue was essential for the PKC ϵ mediated membrane accumulation of PSD-95. *In vitro*, PKC ϵ phosphorylated both PSD-95 and JNK1. The JNK1 inhibitor also prevented PKC ϵ activation-mediated increase in p-PSD-95^{S295}, confirming previous findings showing that serine-295 phosphorylation of PSD-95 is regulated by Rac1-JNK1 and PP1/PP2A signaling (33,54). PKC ϵ is involved in JNK activation; PKD, a downstream effector of PKC, also regulates JNK (38-39,55). Knockdown of either PKC ϵ or JNK inhibited the PKC ϵ activator mediated p-PSD-95^{S295} accumulation in the membrane, thus confirming that PKC ϵ and JNK act collectively in regulating PSD-95. Although it has been reported that synaptic localization of PSD-95 is regulated by JNK signaling and not by CaMKII (33,56), our data demonstrate a role of both JNK1 and CaMKII. This is possible as PKC activation induces a simultaneous translocation of calcium/calmodulin-dependent kinase II (CaMKII) to synapses (21) and CaMKII activation is needed for PSD-95-induced synaptic strengthening (22). CaMKII is a downstream target of PKC ϵ in many pathways, including the events responsible for the induction of neuroplastic changes associated with hyperalgesic priming (57). In this study, we found that both JNK1 and CaMKII inhibitors prevented the PKC ϵ mediated membrane association of p-PSD-95^{S295}. These results suggest that JNK1 and CaMKII are downstream to PKC ϵ in events responsible for phosphorylation and membrane accumulation of PSD-95.

We also demonstrated that PKC ϵ activation increases the levels of PSD-95 and the number of synapses. In adult hippocampal slices, bryostatin 1 increased basal synaptic activity. Our results indicate an important link between PKC ϵ activation and the membrane localization of PSD-95, specifically enriching the membrane with the p-PSD-95^{S295} form, which is known to strengthen the excitatory synapses (33). PSD-95 also regulates membrane insertion of AMPA receptor and dendritic spine morphology during synaptic plasticity (22,30-32).

Overexpression of PSD-95 converts silent synapses to functional synapses (58), while synaptophysin may be required for increased presynaptic vesicle density, thereby facilitating neurotransmitter release (59). We found that overexpressing PKC ϵ in primary human neurons induces the mRNA and protein levels of PSD-95 and synaptophysin, while knockdown of PKC ϵ reduces PSD-95 and synaptophysin mRNA and protein levels. Our results indicate that PKC ϵ regulates the gene expression of PSD-95 and synaptophysin. PKC ϵ may play a critical role synapse maintenance by regulating the synthesis of PSD-95 and synaptophysin (18). PKC ϵ is known to drive the mitogenic response and DNA synthesis (60) via the Raf-MEK-ERK cascade and regulates transcription of essential genes through JNK/AP1, NF- κ B and JAK/STAT cascades (61-62). PSD-95 is a critical transcriptional target of NF- κ B, which is known to induce excitatory synapse formation and regulate dendritic spine formation and morphology in murine hippocampal neurons (63). Synaptophysin mRNA expression is induced by the BDNF-cFos pathway (64). NF- κ B and synaptophysin have a common regulator in BDNF (65). PKC ϵ upregulates BDNF expression (19-20,66).

In conclusion, PKC ϵ has two specific roles in synaptogenesis: at the postsynaptic site it regulates PSD-95, either directly or through JNK1 and CaMKII, and at the presynaptic site it induces the expression of synaptophysin. Repeated treatment with PKC ϵ activators induces synthesis of PKC ϵ , PSD-95 and synaptophysin, resulting in an increased number of synapses. PKC ϵ knockdown inhibits the synthesis of PSD-95 and synaptophysin leading to a reduced number of synapses. Besides the PKC-JNK1/CaMKII- PSD-95 pathway, PKC ϵ can also induce synaptogenesis through the HuD-BDNF pathway. PKC ϵ stabilizes HuD, which increases the stability and rate of translocation of target mRNAs. HuD increases as a result of PKC ϵ activation after learning (67) and stabilizes the mRNA for BDNF, nerve growth factor (NGF), and neurotrophin-3 (NT-3) (19). PKC ϵ activation induces the synthesis of BDNF (10,20,47) and BDNF induces transport of PSD-95 to the dendrites (68), which is required for maintenance of mature spines (69). Deficits of PKC ϵ function could also contribute to the synapse loss in AD (15), while the therapeutic

elimination of such deficits may offer a strategy for the treatment of synaptic loss in AD and other synaptic disorders.

EXPERIMENTAL PROCEDURES

Materials—Bryostatin 1 was purchased from Biomol International (Farmingdale, NY, USA). DCPLA methyl ester (DCPLA-ME) was synthesized in our laboratory following the method described earlier (34,70) and shown to be specific for PKC ϵ . Primary antibodies (rabbit polyclonal anti-PKC ϵ (sc-214), rabbit polyclonal anti-PKC α (sc-208), rabbit polyclonal anti-PKC δ (sc-213), mouse monoclonal anti-synaptophysin (sc-17750) and mouse monoclonal anti- β -actin (sc-47778)) were obtained from Santa Cruz Biotechnology, Inc. (Santa Cruz, CA, USA). Rabbit polyclonal anti-synaptophysin (TA300431) and rabbit polyclonal anti-phospho-PSD-95 (serine-295) (TA303850) were obtained from Origene (Rockville, MD, USA) and rabbit polyclonal anti-PSD-95 (#3450) and rabbit polyclonal anti-JNK1/2 (#9258) were obtained from Cell Signaling Technology, Inc (Danvers, MA, USA). Chicken polyclonal anti-NeuN (ab134014) was obtained from Abcam (Cambridge, MA, USA). All secondary antibodies were purchased from Jackson ImmunoResearch Laboratories, Inc (Bar Harbor, ME, USA). The anti-chicken Cy5 conjugated antibody was purchased from Abcam (Cambridge, MA, USA). Bisindolylmaleimide I (Go 6850) and PKC ϵ translocation inhibitor [EAVSLKPT] were obtained from Santa Cruz Biotechnology, Inc (Santa Cruz, CA, USA) and SP600125 and KN-93 were obtained from Cell Signaling Technology, Inc (Danvers, MA, USA).

Cell culture—Human primary neurons (Hippocampal neurons, Catalog No: 1540, ScienCell Research Laboratories, Carlsbad, CA, USA) were plated on poly-L-lysine coated plates and were maintained in neuronal medium (ScienCell) supplemented with the neuronal growth supplement (NGS, ScienCell). For maintenance of neurons half of the media was changed every 3 days. Fresh activators were added with every media change. Human HEK-293 cells were obtained from ATCC, Manassas, VA, USA. Cells were maintained in EMEM and 10% fetal bovine serum (FBS).

Organotypic slice culture—Organotypic hippocampal slices were prepared mainly according to the method described by Stoppini et al. (71) with slight modifications (72). Rats were sacrificed and immediately decapitated under sterile conditions. Brains were rapidly removed and placed into a chilled dissection medium (DM) composed of Hibernate A (BrainBits, Springfield, IL), 2% B27 supplement, 2 mM L-glutamine by GlutaMax and antibiotic–antimycotics (all from Invitrogen, Carlsbad, CA, USA). The hippocampi were dissected out in fresh chilled dissection medium. Isolated hippocampi were washed in new chilled DM and placed on a wet 3 mm paper on the Teflon stage of a manual tissue slice chopper (Vibratome Co., Saint Louis, MO, USA) for coronal sectioning at 300 μ m. Each slice with intact pyramidal and granular layers was transferred to one membrane insert (Millipore, Bedford, MA, USA) in 12-well plates containing Neurobasal A, 20% horse serum, 2 mM l-glutamine, and antibiotics–antimycotics for four days. For long term maintenance slices were cultured in serum-free medium consisting of Neurobasal A with 2% B27, 2 mM l-glutamine, and antibiotic–antimycotics. Slices were incubated in a humidified 5% CO₂ atmosphere at 37 °C. The entire medium was replaced with fresh medium at day 1. After that, half the medium was removed and replaced with fresh medium twice a week.

Cell lysis and Western blot analysis—Cells were harvested in homogenizing buffer (HB) containing 10mM Tris-Cl (pH 7.4), 1 mM PMSF (phenylmethylsulfonylfluoride), 1 mM EGTA, 1 mM EDTA, 50 mM NaF and 20 μ M leupeptin, and were lysed by sonication. The homogenate was centrifuged at 100,000 \times g for 15 min at 4°C to obtain the cytosolic fraction (soluble) and membrane (particulate). The pellet was resuspended in the HB by sonication. For whole cell protein isolation from primary neurons the HB contained 1% Triton X-100. Protein concentration was measured using the Coomassie Plus (Bradford) Protein Assay kit (Pierce, Rockford, IL, USA). Following quantification, 20 μ g of protein from each sample was subjected to SDS-PAGE analysis in a 4-20% gradient Tris-glycine polyacrylamide gel (Invitrogen, Carlsbad, CA, USA). The separated protein was then transferred to a nitrocellulose membrane. The membrane was blocked with BSA and incubated with primary

antibody overnight at 4°C. All the primary antibodies were used at 1:1000 dilution except rabbit polyclonal anti-p-PSD-95^{S295} (1:10000) and rabbit polyclonal anti-synaptophysin (1:10000). After incubation, it was washed 3× with TBS-T (Tris-buffered saline-Tween 20) and further incubated with alkaline phosphatase conjugated secondary antibody at 1:10000 dilution for 45 min. The membrane was finally washed 3× with TBS-T and developed using the 1-step NBT-BCIP substrate (Pierce, Rockford, IL, USA). The blot was imaged in an ImageQuant RT-ECL (GE Life Sciences, Piscataway, NJ) and densitometric quantification was performed using IMAL software. For quantifying expression of a protein, the densitometric value for the protein of interest was normalized against β-actin (loading control).

Electrophysiology—Rats (1 month old) were euthanized and hippocampus was isolated and sliced into 300-μm slices on a Leica VT1200S Vibratome. Slices were incubated in ACSF at room temperature for one hour until recording. The ACSF contains (mM): NaCl (124), KCl (3), MgSO₄ (1.2), CaCl₂ (2.1), Na₂ PO₄ (1.4), NaHCO₂ (26), Dextrose (20) and is saturated with 95% O₂ and 5% CO₂ which maintains the pH at 7.4. Slices were treated with ethanol or bryostatin 1 for 1hr or 4hr. All recordings were made at room temperature. For synaptic stimulation and field excitatory synaptic potentials (EPSP) recordings pyramidal neurons in the CA1 field were identified with an Olympus BX50WI microscope. Field potential recordings were measured to determine synaptic function. A bipolar stimulating electrode (100-μm separation, FHC, Bowdoinham, ME) was placed in the hippocampal Schaffer collateral pathway to elicit EPSPs in CA1 stratum radiatum, EPSPs were recorded through patch pipettes (2-5 MΩ, 1.5 mm OD, 0.86 mm ID, P87 Brown-Flaming Puller, Sutter Instruments) filled with ACSF. All parameters including pulse duration, width, and frequency were computer controlled. Constant-current pulse intensity was controlled by a stimulus isolation unit. Basal synaptic transmission, represented by input-output responses, was determined by the slopes of stabilized EPSP to different stimulus intensities. The strength of EPSPs was assessed by measuring the slopes (initial 20-80%) of the EPSPs rising phase.

PKC Assay—To measure PKC activity, 100 ng recombinant PKCε (Sigma) was incubated for 15 min at 37°C in the presence of 100ng JNK1 or 100ng PSD-95 or 100 ng CaMKII, 4.89 mM CaCl₂, 1.2 μg/μl phosphatidyl-L-serine, 0.18 μg/μl 1,2-dioctanoyl-*sn*-glycerol, 10 mM MgCl₂, 20 mM HEPES (pH 7.4), 0.8 mM EDTA, 4 mM EGTA, 4% glycerol, 8 μg/ml aprotinin, 8 μg/ml leupeptin, 2 mM benzamidine and 0.5 μCi of [γ-³²P]ATP. [³²P] Phosphoprotein formation was measured by adsorption onto phosphocellulose as described previously (70).

Knockdown and overexpression—Human PSD-95 was cloned into pCDNA3.1 plasmid (Genscript, Piscataway, NJ, USA). Mutant PSD-95 mutated at serine-295 residue was also cloned into pCDNA3.1 plasmid and was obtained from Genscript (Piscataway, NJ, USA). PKCε knockdown was done using PKCε-siRNA constructs purchased from Santa Cruz Biotechnology, Inc (Santa Cruz, CA, USA). JNK knockdown was done using SAPK/JNK-siRNA from Cell Signaling Technology, Inc (Danvers, MA, USA). Overexpression of PKCε was obtained by transfecting pCMV6-ENTRY vector containing human PKCε cDNA (Origene, Rockville, MD, USA). Transfection was done using Lipofectamine 3000 (Invitrogen, Carlsbad, CA, USA). Medium was changed after 6hr of lipofectamine treatment. Protein expression was measured after 72hr of transfection.

QRT-PCR—QRT-PCR was done following the method described earlier (13). Total RNA (500ng) was reverse-transcribed using oligo (dT) and Superscript III (Invitrogen, USA) at 50°C for 1 hr. The cDNA products were analyzed using a LightCycler 480 II (Roche) PCR machine and LightCycler 480 SYBR Green 1 master mix following the manufacturer's protocol. Primers for PKCε (Forward Primer – AGCCTCGTTCACGGTTCTATGC, Reverse primer – GCAGTGACCTTCTGCATCCAGA), PSD-95 (Forward Primer – TCCACTCTGACAGTGAGACCGA, Reverse primer – CGTCACTGTCTCGTAGCTCAGA), synaptophysin (Forward Primer – TCGGCTTTGTGAAGGTGCTGCA, Reverse primer – TCACTCTCGGTCTTGTGGCAC), SNAP-25 (Forward Primer – CGTCGTATGCTGCAACTGGTTG, Reverse primer – GGTTCATGCCTTCTTCGACACG),

Syntaxin-1 (Forward Primer – TGGAGAACAGCATCCGTGAGCT, Reverse primer – CCTCTCCACATAGTCTACCGCG) and GAPDH (Forward Primer – GTCTCCTCTGACTTCAACAGCG, Reverse primer – ACCACCCTGTTGCTGTAGCCAA) were purchased from Origene (Rockville, MD, USA).

Electron microscopy- Electron microscopy of slices were done following methods described earlier (9). Hippocampi were sectioned with a vibratome at 100 μm. Hippocampi were fixed in 1% OsO₄. Electron micrographs (100 μm² CA1 area at ×5,000) were made of Epon-embedded hippocampal sections with a JEOL 200CX electron microscope. These sections were 90 nm thick and had been previously stained with uranyl acetate and lead citrate. During quantification, electron micrographs were digitally zoomed up to ×20,000 magnification. Spines were defined as structures that formed synapses with axon boutons and did not contain mitochondria. Presynaptic vesicle density was measured from within the presynaptic axonal boutons that were seen to form synapses with dendritic spines of diameter larger than 600nm. Increased numbers of presynaptic vesicles in axon boutons were measured as an increase in the frequency of axon boutons with presynaptic vesicles that occupied more than 50% of the cross-section space not occupied by other organelles.

Immunofluorescence and Confocal microscopy—Cells were grown in four-chambered slides (Nunc, USA) at low density. For immunofluorescence staining the cells were washed with PBS (pH 7.4) and fixed with 4% paraformaldehyde for 4 min. Following fixation, cells were blocked and permeabilized with 5% horse serum and 0.3% Triton X-100 in 1× PBS for 30 min. Cells were washed 3 × with 1 × PBS and incubated with primary antibodies (rabbit

polyclonal anti-PSD-95, mouse monoclonal anti-synaptophysin and chicken polyclonal anti-NeuN) for 1hr at 1:100 dilution. After the incubation slides were again washed 3 × in 1 × PBS and were incubated with the FITC anti-rabbit IgG, rhodamine anti-mouse IgG and Cy5 anti-chicken IgY for 1hr at 1:400 dilution. Cells were further washed and mounted in Pro Long Gold antifade mounting solution (Invitrogen, USA). Stained cells were viewed under the LSM 710 Meta confocal microscope (Zeiss) at 350 nm, 490 nm, 540 nm and 650nm excitation and 470 nm, 525 nm, 625 nm and 667nm emission for DAPI, FITC, rhodamine and Cy5 respectively. Six individual fields at 40× or 63× oil lens magnification were analyzed for the mean fluorescence intensity (MFI) in each channel. Punctate colocalization was done following methods described earlier (43-44).

Statistical analysis—All experiments were performed at least three times. Data are represented as mean ± SEM. All data were analyzed by one-way ANOVA and Newman-Keuls multiple comparison post test. Significantly different paired groups were further analyzed by two-tailed Student's *t*-test using GraphPad Prism 6.1 software (La Jolla, CA, USA). P values < 0.05 were considered statistically significant.

CONFLICT OF INTEREST

The authors declare no competing financial interests.

AUTHORSHIP STATEMENT

AS, TJN and DLA designed the study and wrote the paper. AS performed and analyzed all the biochemical and immunofluorescence experiments, JH performed and analyzed all the electron microscopy data and DW performed and analyzed the electrophysiology experiments.

REFERENCES

1. Akita, Y. (2002) Protein kinase C-epsilon (PKC-epsilon): its unique structure and function. *J Biochem* **132**, 847-852
2. Chen, Y., and Tian, Q. (2011) The role of protein kinase C epsilon in neural signal transduction and neurogenic diseases. *Front Med* **5**, 70-76

3. Zeidman, R., Lofgren, B., Pahlman, S., and Larsson, C. (1999) PKCepsilon, via its regulatory domain and independently of its catalytic domain, induces neurite-like processes in neuroblastoma cells. *J Cell Biol* **145**, 713-726
4. Fagerstrom, S., Pahlman, S., Gestblom, C., and Nanberg, E. (1996) Protein kinase C-epsilon is implicated in neurite outgrowth in differentiating human neuroblastoma cells. *Cell Growth Differ* **7**, 775-785
5. Prekeris, R., Hernandez, R. M., Mayhew, M. W., White, M. K., and Terrian, D. M. (1998) Molecular analysis of the interactions between protein kinase C-epsilon and filamentous actin. *J Biol Chem* **273**, 26790-26798
6. Prekeris, R., Mayhew, M. W., Cooper, J. B., and Terrian, D. M. (1996) Identification and localization of an actin-binding motif that is unique to the epsilon isoform of protein kinase C and participates in the regulation of synaptic function. *J Cell Biol* **132**, 77-90
7. Bank, B., DeWeer, A., Kuzirian, A. M., Rasmussen, H., and Alkon, D. L. (1988) Classical conditioning induces long-term translocation of protein kinase C in rabbit hippocampal CA1 cells. *Proc Natl Acad Sci U S A* **85**, 1988-1992
8. Olds, J. L., Anderson, M. L., McPhie, D. L., Staten, L. D., and Alkon, D. L. (1989) Imaging of memory-specific changes in the distribution of protein kinase C in the hippocampus. *Science* **245**, 866-869
9. Hongpaisan, J., and Alkon, D. L. (2007) A structural basis for enhancement of long-term associative memory in single dendritic spines regulated by PKC. *Proc Natl Acad Sci U S A* **104**, 19571-19576
10. Hongpaisan, J., Sun, M. K., and Alkon, D. L. (2011) PKC epsilon activation prevents synaptic loss, Abeta elevation, and cognitive deficits in Alzheimer's disease transgenic mice. *J Neurosci* **31**, 630-643
11. Alkon, D. L., and Rasmussen, H. (1988) A spatial-temporal model of cell activation. *Science* **239**, 998-1005
12. Nelson, T. J., Collin, C., and Alkon, D. L. (1990) Isolation of a G protein that is modified by learning and reduces potassium currents in Hermissenda. *Science* **247**, 1479-1483
13. Sen, A., Alkon, D. L., and Nelson, T. J. (2012) Apolipoprotein E3 (ApoE3) but not ApoE4 protects against synaptic loss through increased expression of protein kinase C epsilon. *J Biol Chem* **287**, 15947-15958
14. Hama, H., Hara, C., Yamaguchi, K., and Miyawaki, A. (2004) PKC signaling mediates global enhancement of excitatory synaptogenesis in neurons triggered by local contact with astrocytes. *Neuron* **41**, 405-415
15. Khan, T. K., Sen, A., Hongpaisan, J., Lim, C. S., Nelson, T. J., and Alkon, D. L. (2015) PKCepsilon Deficits in Alzheimer's Disease Brains and Skin Fibroblasts. *J Alzheimers Dis* **43**, 491-509
16. Lin, D. T., Makino, Y., Sharma, K., Hayashi, T., Neve, R., Takamiya, K., and Huganir, R. L. (2009) Regulation of AMPA receptor extrasynaptic insertion by 4.1N, phosphorylation and palmitoylation. *Nat Neurosci* **12**, 879-887
17. Gomes, A. R., Correia, S. S., Esteban, J. A., Duarte, C. B., and Carvalho, A. L. (2007) PKC anchoring to GluR4 AMPA receptor subunit modulates PKC-driven receptor phosphorylation and surface expression. *Traffic* **8**, 259-269
18. Alkon, D. L., Epstein, H., Kuzirian, A., Bennett, M. C., and Nelson, T. J. (2005) Protein synthesis required for long-term memory is induced by PKC activation on days before associative learning. *Proc Natl Acad Sci U S A* **102**, 16432-16437
19. Lim, C. S., and Alkon, D. L. (2012) Protein kinase C stimulates HuD-mediated mRNA stability and protein expression of neurotrophic factors and enhances dendritic maturation of hippocampal neurons in culture. *Hippocampus* **22**, 2303-2319
20. Sen, A., Nelson, T. J., and Alkon, D. L. (2015) ApoE4 and Abeta Oligomers Reduce BDNF Expression via HDAC Nuclear Translocation. *J Neurosci* **35**, 7538-7551

21. Fong, D. K., Rao, A., Crump, F. T., and Craig, A. M. (2002) Rapid synaptic remodeling by protein kinase C: reciprocal translocation of NMDA receptors and calcium/calmodulin-dependent kinase II. *J Neurosci* **22**, 2153-2164
22. Zhang, P., and Lisman, J. E. (2012) Activity-dependent regulation of synaptic strength by PSD-95 in CA1 neurons. *J Neurophysiol* **107**, 1058-1066
23. Yan, J. Z., Xu, Z., Ren, S. Q., Hu, B., Yao, W., Wang, S. H., Liu, S. Y., and Lu, W. (2011) Protein kinase C promotes N-methyl-D-aspartate (NMDA) receptor trafficking by indirectly triggering calcium/calmodulin-dependent protein kinase II (CaMKII) autophosphorylation. *J Biol Chem* **286**, 25187-25200
24. Nelson, T. J., and Alkon, D. L. (2014) Molecular regulation of synaptogenesis during associative learning and memory. *Brain Res*
25. Sun, M. K., Nelson, T. J., and Alkon, D. L. (2015) Towards universal therapeutics for memory disorders. *Trends Pharmacol Sci*
26. Li, Z., and Sheng, M. (2003) Some assembly required: the development of neuronal synapses. *Nat Rev Mol Cell Biol* **4**, 833-841
27. Sheng, M., and Hoogenraad, C. C. (2007) The postsynaptic architecture of excitatory synapses: a more quantitative view. *Annu Rev Biochem* **76**, 823-847
28. Funke, L., Dakoji, S., and Brecht, D. S. (2005) Membrane-associated guanylate kinases regulate adhesion and plasticity at cell junctions. *Annu Rev Biochem* **74**, 219-245
29. Bats, C., Groc, L., and Choquet, D. (2007) The interaction between Stargazin and PSD-95 regulates AMPA receptor surface trafficking. *Neuron* **53**, 719-734
30. Ehrlich, I., Klein, M., Rumpel, S., and Malinow, R. (2007) PSD-95 is required for activity-driven synapse stabilization. *Proc Natl Acad Sci U S A* **104**, 4176-4181
31. El-Husseini, A. E., Schnell, E., Chetkovich, D. M., Nicoll, R. A., and Brecht, D. S. (2000) PSD-95 involvement in maturation of excitatory synapses. *Science* **290**, 1364-1368
32. De Roo, M., Klauser, P., Mendez, P., Poglia, L., and Muller, D. (2008) Activity-dependent PSD formation and stabilization of newly formed spines in hippocampal slice cultures. *Cereb Cortex* **18**, 151-161
33. Kim, M. J., Futai, K., Jo, J., Hayashi, Y., Cho, K., and Sheng, M. (2007) Synaptic accumulation of PSD-95 and synaptic function regulated by phosphorylation of serine-295 of PSD-95. *Neuron* **56**, 488-502
34. Kanno, T., Yamamoto, H., Yaguchi, T., Hi, R., Mukasa, T., Fujikawa, H., Nagata, T., Yamamoto, S., Tanaka, A., and Nishizaki, T. (2006) The linoleic acid derivative DCP-LA selectively activates PKC-epsilon, possibly binding to the phosphatidylserine binding site. *J Lipid Res* **47**, 1146-1156
35. Sun, M. K., Hongpaisan, J., Nelson, T. J., and Alkon, D. L. (2008) Poststroke neuronal rescue and synaptogenesis mediated in vivo by protein kinase C in adult brains. *Proc Natl Acad Sci U S A* **105**, 13620-13625
36. Nelson, T. J., and Alkon, D. L. (2009) Neuroprotective versus tumorigenic protein kinase C activators. *Trends Biochem Sci* **34**, 136-145
37. Steinberg, S. F. (2008) Structural basis of protein kinase C isoform function. *Physiol Rev* **88**, 1341-1378
38. Comalada, M., Xaus, J., Valledor, A. F., Lopez-Lopez, C., Pennington, D. J., and Celada, A. (2003) PKC epsilon is involved in JNK activation that mediates LPS-induced TNF-alpha, which induces apoptosis in macrophages. *Am J Physiol Cell Physiol* **285**, C1235-1245
39. Lang, W., Wang, H., Ding, L., and Xiao, L. (2004) Cooperation between PKC-alpha and PKC-epsilon in the regulation of JNK activation in human lung cancer cells. *Cell Signal* **16**, 457-467
40. Brooks, I. M., and Tavalin, S. J. (2011) Ca²⁺/calmodulin-dependent protein kinase II inhibitors disrupt AKAP79-dependent PKC signaling to GluA1 AMPA receptors. *J Biol Chem* **286**, 6697-6706

41. Waxham, M. N., and Aronowski, J. (1993) Ca²⁺/calmodulin-dependent protein kinase II is phosphorylated by protein kinase C in vitro. *Biochemistry* **32**, 2923-2930
42. Tokuda, K., Izumi, Y., and Zorumski, C. F. (2013) Locally-generated acetaldehyde is involved in ethanol-mediated LTP inhibition in the hippocampus. *Neurosci Lett* **537**, 40-43
43. Barker, A. J., Koch, S. M., Reed, J., Barres, B. A., and Ullian, E. M. (2008) Developmental control of synaptic receptivity. *J Neurosci* **28**, 8150-8160
44. Ippolito, D. M., and Eroglu, C. (2010) Quantifying synapses: an immunocytochemistry-based assay to quantify synapse number. *J Vis Exp*
45. Kortmansky, J., and Schwartz, G. K. (2003) Bryostatin-1: a novel PKC inhibitor in clinical development. *Cancer Invest* **21**, 924-936
46. Nelson, T. J., Sen, A., Alkon, D. L., and Sun, M. K. (2014) Adduct formation in liquid chromatography-triple quadrupole mass spectrometric measurement of bryostatin 1. *J Chromatogr B Analyt Technol Biomed Life Sci* **944**, 55-62
47. Hongpaisan, J., Xu, C., Sen, A., Nelson, T. J., and Alkon, D. L. (2013) PKC activation during training restores mushroom spine synapses and memory in the aged rat. *Neurobiol Dis* **55**, 44-62
48. Cheng, D., Hoogenraad, C. C., Rush, J., Ramm, E., Schlager, M. A., Duong, D. M., Xu, P., Wijayawardana, S. R., Hanfelt, J., Nakagawa, T., Sheng, M., and Peng, J. (2006) Relative and absolute quantification of postsynaptic density proteome isolated from rat forebrain and cerebellum. *Mol Cell Proteomics* **5**, 1158-1170
49. Kim, E., and Sheng, M. (2004) PDZ domain proteins of synapses. *Nat Rev Neurosci* **5**, 771-781
50. Bell, K. F., and Hardingham, G. E. (2011) The influence of synaptic activity on neuronal health. *Curr Opin Neurobiol* **21**, 299-305
51. Lipsky, R. H., and Marini, A. M. (2007) Brain-derived neurotrophic factor in neuronal survival and behavior-related plasticity. *Ann N Y Acad Sci* **1122**, 130-143
52. Soriano, F. X., Papadia, S., Hofmann, F., Hardingham, N. R., Bading, H., and Hardingham, G. E. (2006) Preconditioning doses of NMDA promote neuroprotection by enhancing neuronal excitability. *J Neurosci* **26**, 4509-4518
53. Akers, R. F., Lovinger, D. M., Colley, P. A., Linden, D. J., and Routtenberg, A. (1986) Translocation of protein kinase C activity may mediate hippocampal long-term potentiation. *Science* **231**, 587-589
54. Yang, H., Courtney, M. J., Martinsson, P., and Manahan-Vaughan, D. (2011) Hippocampal long-term depression is enhanced, depotentiation is inhibited and long-term potentiation is unaffected by the application of a selective c-Jun N-terminal kinase inhibitor to freely behaving rats. *Eur J Neurosci* **33**, 1647-1655
55. Hurd, C., Waldron, R. T., and Rozengurt, E. (2002) Protein kinase D complexes with C-Jun N-terminal kinase via activation loop phosphorylation and phosphorylates the C-Jun N-terminus. *Oncogene* **21**, 2154-2160
56. Farias, G. G., Alfaro, I. E., Cerpa, W., Grabowski, C. P., Godoy, J. A., Bonansco, C., and Inestrosa, N. C. (2009) Wnt-5a/JNK signaling promotes the clustering of PSD-95 in hippocampal neurons. *J Biol Chem* **284**, 15857-15866
57. Ferrari, L. F., Bogen, O., and Levine, J. D. (2013) Role of nociceptor alphaCaMKII in transition from acute to chronic pain (hyperalgesic priming) in male and female rats. *J Neurosci* **33**, 11002-11011
58. Stein, V., House, D. R., Bredt, D. S., and Nicoll, R. A. (2003) Postsynaptic density-95 mimics and occludes hippocampal long-term potentiation and enhances long-term depression. *J Neurosci* **23**, 5503-5506
59. Sun, M. K., and Alkon, D. L. (2009) Protein kinase C activators as synaptogenic and memory therapeutics. *Arch Pharm (Weinheim)* **342**, 689-698
60. Li, Y., Davis, K. L., and Sytkowski, A. J. (1996) Protein kinase C-epsilon is necessary for erythropoietin's up-regulation of c-myc and for factor-dependent DNA synthesis. Evidence for discrete signals for growth and differentiation. *J Biol Chem* **271**, 27025-27030

61. Caino, M. C., von Burstin, V. A., Lopez-Haber, C., and Kazanietz, M. G. (2011) Differential regulation of gene expression by protein kinase C isozymes as determined by genome-wide expression analysis. *J Biol Chem* **286**, 11254-11264
62. Mischak, H., Goodnight, J. A., Kolch, W., Martiny-Baron, G., Schaehtle, C., Kazanietz, M. G., Blumberg, P. M., Pierce, J. H., and Mushinski, J. F. (1993) Overexpression of protein kinase C-delta and -epsilon in NIH 3T3 cells induces opposite effects on growth, morphology, anchorage dependence, and tumorigenicity. *J Biol Chem* **268**, 6090-6096
63. Boersma, M. C., Dresselhaus, E. C., De Biase, L. M., Mihalas, A. B., Bergles, D. E., and Meffert, M. K. (2011) A requirement for nuclear factor-kappaB in developmental and plasticity-associated synaptogenesis. *J Neurosci* **31**, 5414-5425
64. Coffey, E. T., Akerman, K. E., and Courtney, M. J. (1997) Brain derived neurotrophic factor induces a rapid upregulation of synaptophysin and tau proteins via the neurotrophin receptor TrkB in rat cerebellar granule cells. *Neurosci Lett* **227**, 177-180
65. Kajiya, M., Shiba, H., Fujita, T., Takeda, K., Uchida, Y., Kawaguchi, H., Kitagawa, M., Takata, T., and Kurihara, H. (2009) Brain-derived neurotrophic factor protects cementoblasts from serum starvation-induced cell death. *J Cell Physiol* **221**, 696-706
66. Sun, M. K., Hongpaisan, J., Lim, C. S., and Alkon, D. L. (2014) Bryostatin-1 restores hippocampal synapses and spatial learning and memory in adult fragile x mice. *J Pharmacol Exp Ther* **349**, 393-401
67. Pascale, A., Gusev, P. A., Amadio, M., Dottorini, T., Govoni, S., Alkon, D. L., and Quattrone, A. (2004) Increase of the RNA-binding protein HuD and posttranscriptional up-regulation of the GAP-43 gene during spatial memory. *Proc Natl Acad Sci U S A* **101**, 1217-1222
68. Yoshii, A., and Constantine-Paton, M. (2007) BDNF induces transport of PSD-95 to dendrites through PI3K-AKT signaling after NMDA receptor activation. *Nat Neurosci* **10**, 702-711
69. Kellner, Y., Godecke, N., Dierkes, T., Thieme, N., Zagrebelsky, M., and Korte, M. (2014) The BDNF effects on dendritic spines of mature hippocampal neurons depend on neuronal activity. *Front Synaptic Neurosci* **6**, 5
70. Nelson, T. J., Cui, C., Luo, Y., and Alkon, D. L. (2009) Reduction of beta-amyloid levels by novel protein kinase C(epsilon) activators. *J Biol Chem* **284**, 34514-34521
71. Stoppini, L., Buchs, P. A., and Muller, D. (1991) A simple method for organotypic cultures of nervous tissue. *J Neurosci Methods* **37**, 173-182
72. Kim, H., Kim, E., Park, M., Lee, E., and Namkoong, K. (2013) Organotypic hippocampal slice culture from the adult mouse brain: a versatile tool for translational neuropsychopharmacology. *Prog Neuropsychopharmacol Biol Psychiatry* **41**, 36-43
73. Harris, K. M., Jensen, F. E., and Tsao, B. (1992) Three-dimensional structure of dendritic spines and synapses in rat hippocampus (CA1) at postnatal day 15 and adult ages: implications for the maturation of synaptic physiology and long-term potentiation. *J Neurosci* **12**, 2685-2705

Figure Legends:

Fig. 1: PKC ϵ activation prevents degeneration of human primary neurons. Primary human neurons were treated with either DCPLA-ME (100 nM) or bryostatin 1 (0.27 nM) for 40 days. Fresh drug was added every third day with 50% media change. **A.** Image of 40 day old untreated (Control), bryostatin 1 and DCPLA-ME treated neurons. **B.** Number of neurite positive cells counted from three 20 \times fields (508 μm^2) over time. DCPLA-ME and bryostatin 1 treatment stabilized cellular viability for at least 40 days. Viability of untreated cells declined after 20 days. **C-E.** PKC ϵ , PSD-95 and synaptophysin mRNA levels in 40 day old neurons compared to 1 day neurons. **F.** Immunoblot analysis of PKC ϵ , p-PSD-95^{S295}, PSD-95 and synaptophysin in 40 day old neurons compared to 1 day neurons. **G-J.** Immunostaining of p-PSD-95^{S295}, PSD-95 and synaptophysin calculated from immunoblots. Staining is significantly higher in DCPLA-ME and bryostatin 1 treated cells. Data are represented as mean \pm SE of three independent experiments (Student's t-test, * P <0.05 and ** P <0.005).

Fig. 2: PKC ϵ activation induces membrane accumulation of p-PSD-95^{S295}. Primary human neurons were treated with ethanol (C), bryostatin 1 (0.27nM) or DCPLA-ME (100nM) for 1hr, 4hr and 24hr. Neurons were separated into soluble (S) and membrane (P) fractions and immunoblotted against PKC α , PKC ϵ and PKC δ . **(A-C)** and p-PSD-95^{S295}, PSD-95 and β -actin **(E)**. 'M' represent molecular weight marker. PKC activation is reported as the percentage of total protein in the membrane. Bryostatin 1-treated neurons showed PKC ϵ activation at 1hr (175.2 \pm 9.5 %; P =0.002), 4hr (181.6 \pm 10.2 %; P =0.0016) and 24hr (170.9 \pm 7.4 %; P =0.001) compared to the untreated neurons (100.0 \pm 3.1%; $F_{(3,8)}$ =22.5; ANOVA, P <0.0005) **(B)** and DCPLA-ME treated neurons showed a significant increase in PKC ϵ activation at 1hr (144.0 \pm 6.8 %; P =0.004), 4hr (146.5 \pm 6.8 %; P =0.003) and 24hr (133.6 \pm 4.2 %; P =0.003) compared to the untreated neurons ($F_{(3,8)}$ =15.7; ANOVA, P =0.001) **(D)** induced PKC ϵ activation at 1hr, 4hr and 24hr. PKC ϵ activation significantly increased the p-PSD-95^{S295} expression in the membranes at 1hr and 4hr **(F)**. Adult rat hippocampal organotypic slices were treated with ethanol (C), bryostatin 1 (0.27nM) or DCPLA-ME (100nM) for 1hr, 4hr and 24hr. Protein lysates were immunoblotted against p-PSD-95^{S295}, PSD-95 and β -actin. 'M' represent molecular weight marker **(G)**. PKC ϵ activation significantly increased the p-PSD-95^{S295} expression in the membranes at 1hr and 4hr **(H)**. Data are represented as mean \pm SE of three independent experiments (Student's t-test, * P <0.05 and ** P <0.005).

Fig. 3: PKC ϵ mediated phosphorylation of PSD-95 at serine-295 is essential for its membrane accumulation. **A.** Immunoblot representing p-PSD-95^{S295} and PSD-95 expression following incubation of the different combinations of recombinant PKC ϵ , PSD-95, PKC ϵ activators and PKC ϵ inhibitors mentioned above at 37°C for 10 min *in vitro*. **(B).** Bryostatin 1 (0.27nM) and DCPLA-ME (100nM) induces the phosphorylation of PSD-95 at serine-295 position. **C.** Expression of p-PSD-95^{S295} and PSD-95 and β -actin in HEK-293 cells transfected with empty vector, wild type human PSD-95 and mutant PSD-95^{S295K}. **D.** Expression of PSD-95, p-PSD-95^{S295}, PKC ϵ and β -actin in the cytosol and membrane fraction of wild-PSD-95 and PSD-95^{S295K} transfected HEK-293 cells treated with bryostatin 1 and DCPLA-ME for 4hr in presence or absence of EAVSLKPT (5 μ M). Percentage of total protein in the membrane; PKC ϵ **(E)**, PSD-95 **(F)** and p-PSD-95^{S295} **(G)**. Data are represented as mean \pm SE of three independent experiments (Student's t-test, * P <0.05, ** P <0.005 and *** P <0.005).

Fig. 4: PKC ϵ mediated membrane localization of p-PSD-95^{S295} involves JNK1 and CaMKII. Immunoblot showing p-PSD-95^{S295} expression in the membrane of neurons **(A)** treated with vehicle, Bisindolylmaleimide I (100nM, PKC inhibitor), SP600125 (20 μ M, JNK inhibitor) and K-93 (10 μ M, CaMKII inhibitor) for 4hr. **B.** p-PSD-95^{S295} expression in the membrane of neurons treated with DCPLA-ME in presence or absence of different inhibitors. **C.** The inhibitors alone reduced the expression of membrane bound p-PSD-95^{S295}. **D.** PKC, JNK and CaMKII inhibitors prevented the effect of PKC ϵ activation on p-PSD-95. Activated PKC ϵ increases phosphorylation of PSD-95 **(E)**, JNK1 **(F)** and CaMKII **(G)**. **H.** Immunoblot showing the downregulation of PKC ϵ and JNK in PKC ϵ and JNK si-RNA

treated neurons respectively. **I.** Protein expression of p-PSD-95^{S295} and β -actin in the membrane of control, PKC ϵ KD and JNK KD neurons in presence or absence of DCPLA-ME. **J.** Either in PKC ϵ or JNK knockdown human neurons, DCPLA-ME failed to induce the membrane accumulation of p-PSD-95^{S295}. **K.** Diagram representing PKC ϵ mediated membrane translocation of p-PSD-95^{S295} and involvement of JNK1 and CaMKII in the pathway. Data are represented as mean \pm SE of three independent experiments (Student's t-test, * P <0.05 and ** P <0.005).

Fig. 5: PKC ϵ activation induces synaptogenesis. Adult rat hippocampal organotypic slices were treated with ethanol (C), bryostatin 1 (0.27nM) or DCPLA-ME (100nM) for 1hr and 4hr. **A.** Electron micrographs of the stratum radiatum in the hippocampal CA1 area (100 μ m² CA1 area at \times 5,000) treated with bryostatin 1 and DCPLA-ME for 4hr. Thirty to thirty-five CA1 areas each from three different hippocampal slices were analyzed. Dendritic spines showing synapse are highlighted in yellow. **B.** PKC ϵ activation increased the synapse number at 4hr ($F_{(2,96)}=9.05$; ANOVA P < 0.0005) in bryostatin 1 (8.97 ± 0.63 , P < 0.005, $n=34$ CA1 area) and DCPLA-ME (6.97 ± 0.5 ; P < 0.05, $n=30$ CA1 area) treated slices compared to control (5.77 ± 0.50). Typical traces of EPSPs evoked at a stimulus intensity of 200 μ A from bryostatin 1 treated hippocampal slices after 1hr (**C**) and 4hr (**F**). The input–output response, reflecting basal synaptic transmission, increased after treatment with bryostatin1 (0.27 nM), after 1hr (**D**) and 4hr (**G**). Areas under the curves (AUCs) were calculated to compare the basal levels of synaptic transmission. Bryostatin 1 increased EPSP slope significantly at 1hr and 4hr (**E, H**). Data are represented as mean \pm SE of three independent experiments (Student's t-test, * P <0.05 and ** P <0.005).

Fig. 6: PKC ϵ is essential for the expression of PSD-95 and synaptophysin. Primary human neurons were transfected with empty vector /scrambled siRNA (C), PKC ϵ siRNA (PKC ϵ KD), or a PKC ϵ over-expression vector (PKC ϵ OE) following method described in the 'Method' section. Cells were analyzed 72hr after treatment. **A.** mRNA transcript levels of PKC ϵ , **B.** PSD-95, **C.** synaptophysin, **D.** SNAP-25 and **E.** syntaxin-1 in PKC ϵ KD and PKC ϵ OE neurons. PKC ϵ KD suppressed while PKC ϵ OE induced PSD-95 and synaptophysin mRNA transcript. **F.** Agarose gel image showing no effect of scrambled siRNA on PKC ϵ mRNA. **G.** Immunoblot showing protein expression of PKC ϵ in untreated, PKC ϵ siRNA and scrambled siRNA treated human neurons. **H.** Immunoblot staining of PKC ϵ , PSD-95, synaptophysin and actin in control, PKC ϵ KD and PKC ϵ OE neurons. **I, J, K.** Graphical representation of protein expression levels of PKC ϵ , PSD-95, synaptophysin in control, PKC ϵ KD and PKC ϵ OE neurons. Data are represented as mean \pm SE of three independent experiments (Student's t-test, * P <0.05, ** P <0.05 and *** P <0.0005).

Fig. 7: Loss of PKC ϵ prevents synaptogenesis. **A.** Confocal images of untreated, DCPLA-ME (100 nM), bryostatin 1 (0.27 nM), PKC ϵ siRNA + DCPLA-ME (100 nM) and PKC ϵ siRNA + bryostatin 1 (0.27 nM) treated primary human neurons (10 days). Each condition is represented by five panels. Four square panels represents nucleus (blue), PSD-95 (green), synaptophysin (red) and merged image respectively. The rectangular panel represents magnified image of a 40 μ m neurite. **B.** Number of PSD 95 signal grains was measured along 40 μ m neurite length (10 individual neurites from 4 independent slides). Bryostatin 1 and DCPLA-ME significantly increased the PSD-95 clusters per 40 μ m neurite ($F_{(2,9)}=4.5$; ANOVA P <0.05). **C.** Synapses were quantified by the number of colocalized PSD-95 and synaptophysin signals. PKC ϵ activation increased synapse number ($F_{(2,9)}=6.1$; ANOVA P <0.05) and PKC ϵ KO prevented the synaptogenic effect of PKC activators. **D.** Immunoblot analysis of PKC ϵ , p-PSD-95^{S295}, PSD-95 and synaptophysin. PKC ϵ knockdown (KD) reduces PKC ϵ expression by 50% after 10 days in human neurons. **E, F, G.** At 10 days PKC ϵ activation increased the expression of PSD-95 and synaptophysin significantly, but in PKC ϵ KD cells their expressions were lower even after treatment with activators. Data are represented as mean \pm SE of at least three independent experiments (Student's t-test, * P <0.05 and ** P <0.005).

Fig. 8: PKC ϵ activation induces synaptogenesis in hippocampal slices. **A.** Electron microscopy of the hippocampal CA1 area from adult organotypic brain slices treated with vehicle (Control), DCPLA-ME (100 nM) and bryostatin 1 (0.27 nM) for 10days. Dendritic spines showing synapse are highlighted in yellow. **B.** PKC ϵ activation by bryostatin 1 and DCPLA-ME increased synapse number in adult organotypic brain slices ($F_{(2,6)} = 11.9$; ANOVA $P < 0.01$). **C.** Electron micrograph showing increased presynaptic vesicle density in PKC activator treated slices. Grey level of presynaptic vesicle stack from six to seven presynaptic boutons was measured from three different hippocampal slices. “D” represents dendritic spine, red arrow marks synapse and yellow marks presynaptic vesicles. **D.** Bryostatin 1 and DCPLA-ME significantly induced the presynaptic vesicle density at 10 days. Data are represented as mean \pm SE of at least three independent experiments (Student’s t-test, $*P < 0.05$ and $**P < 0.005$).

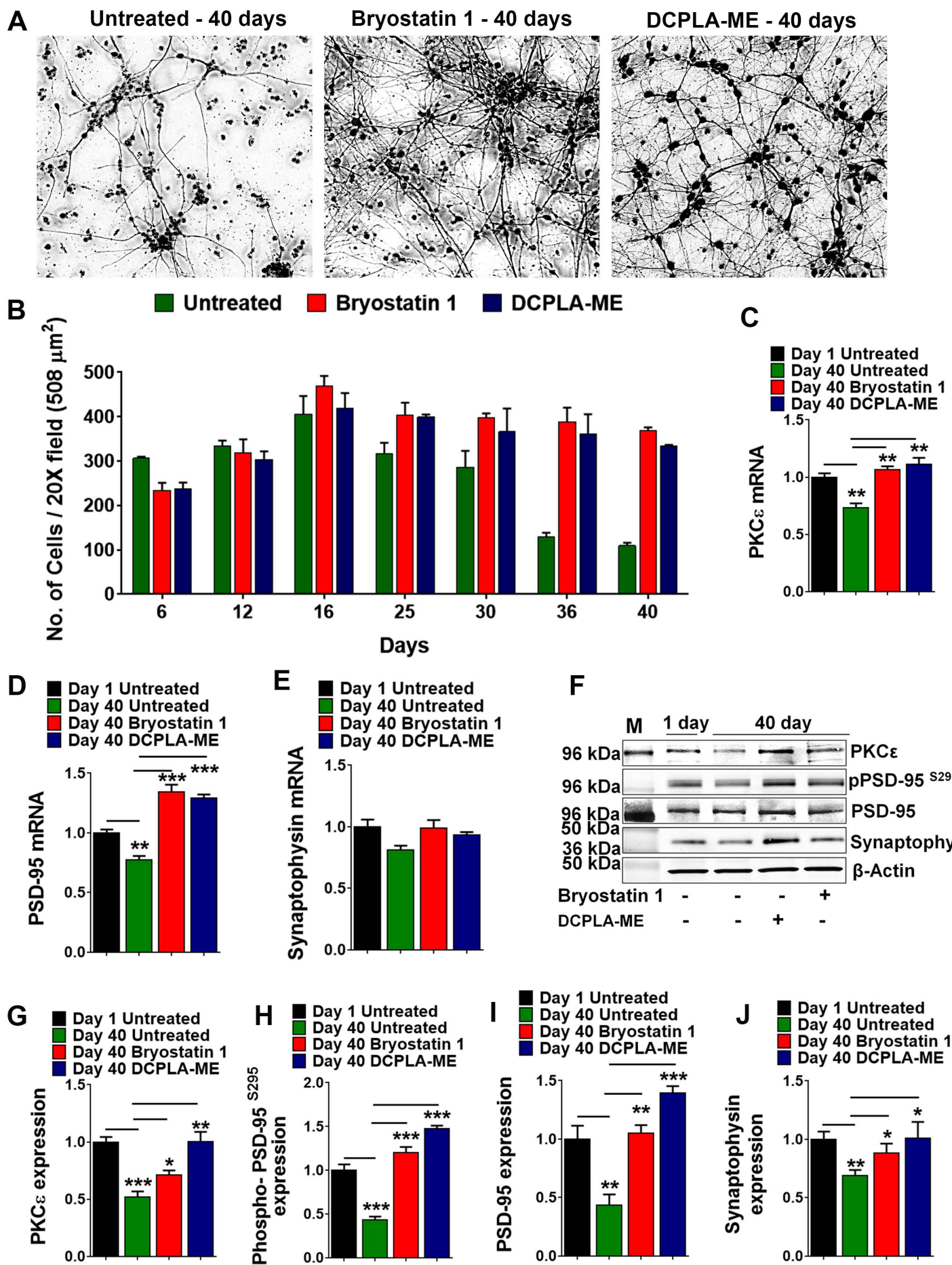


Figure 1

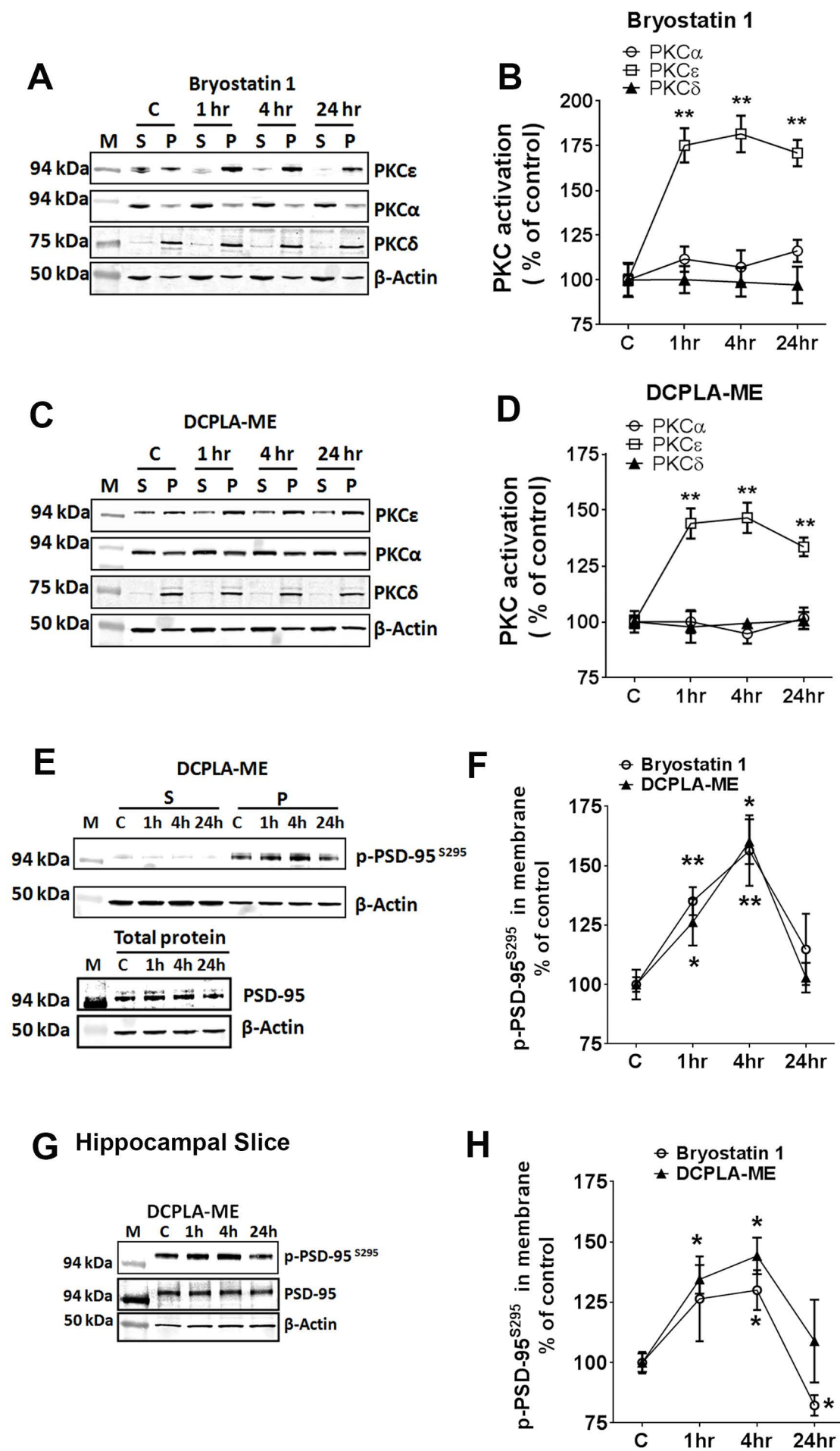


Figure.2

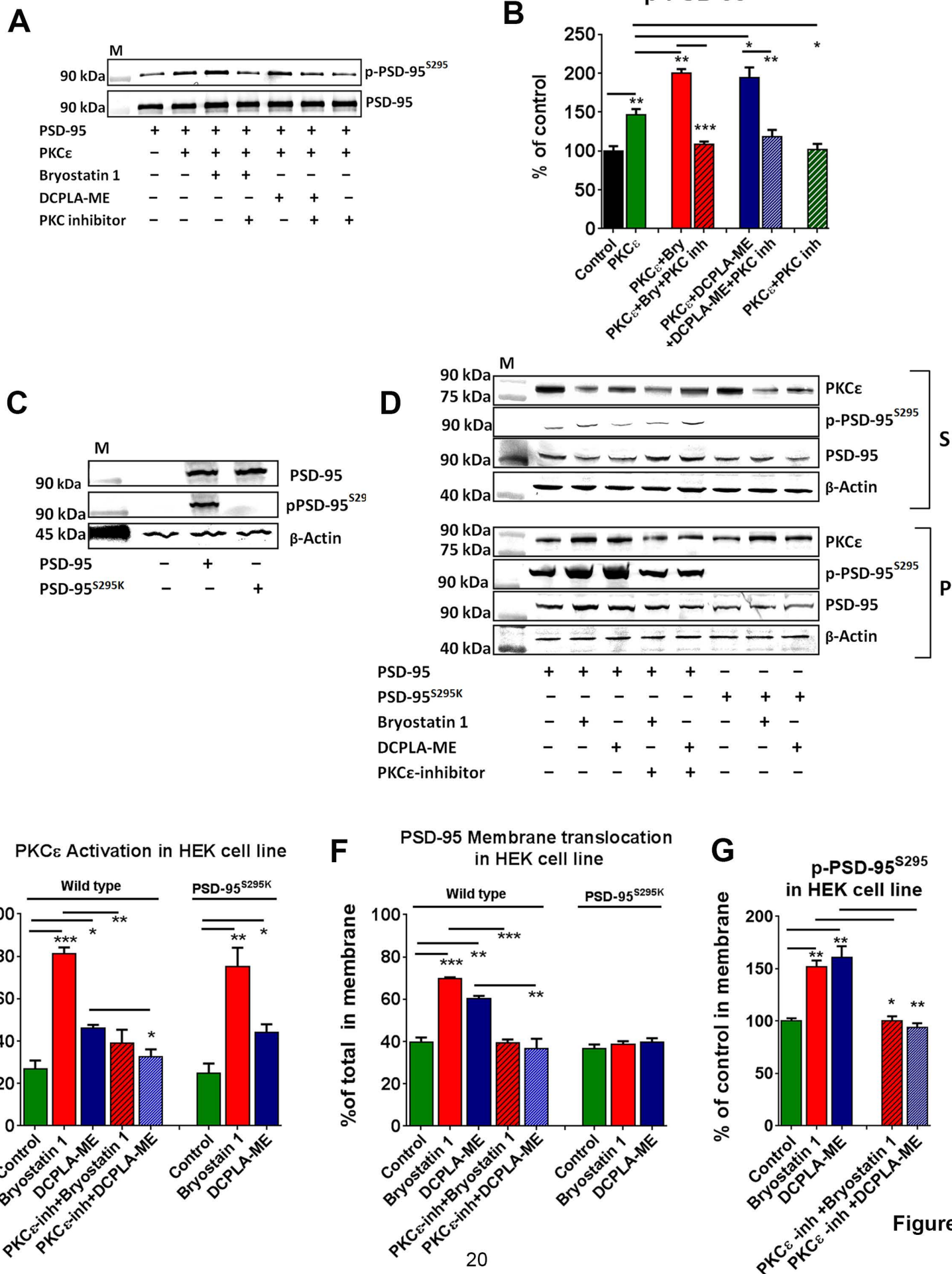


Figure. 3

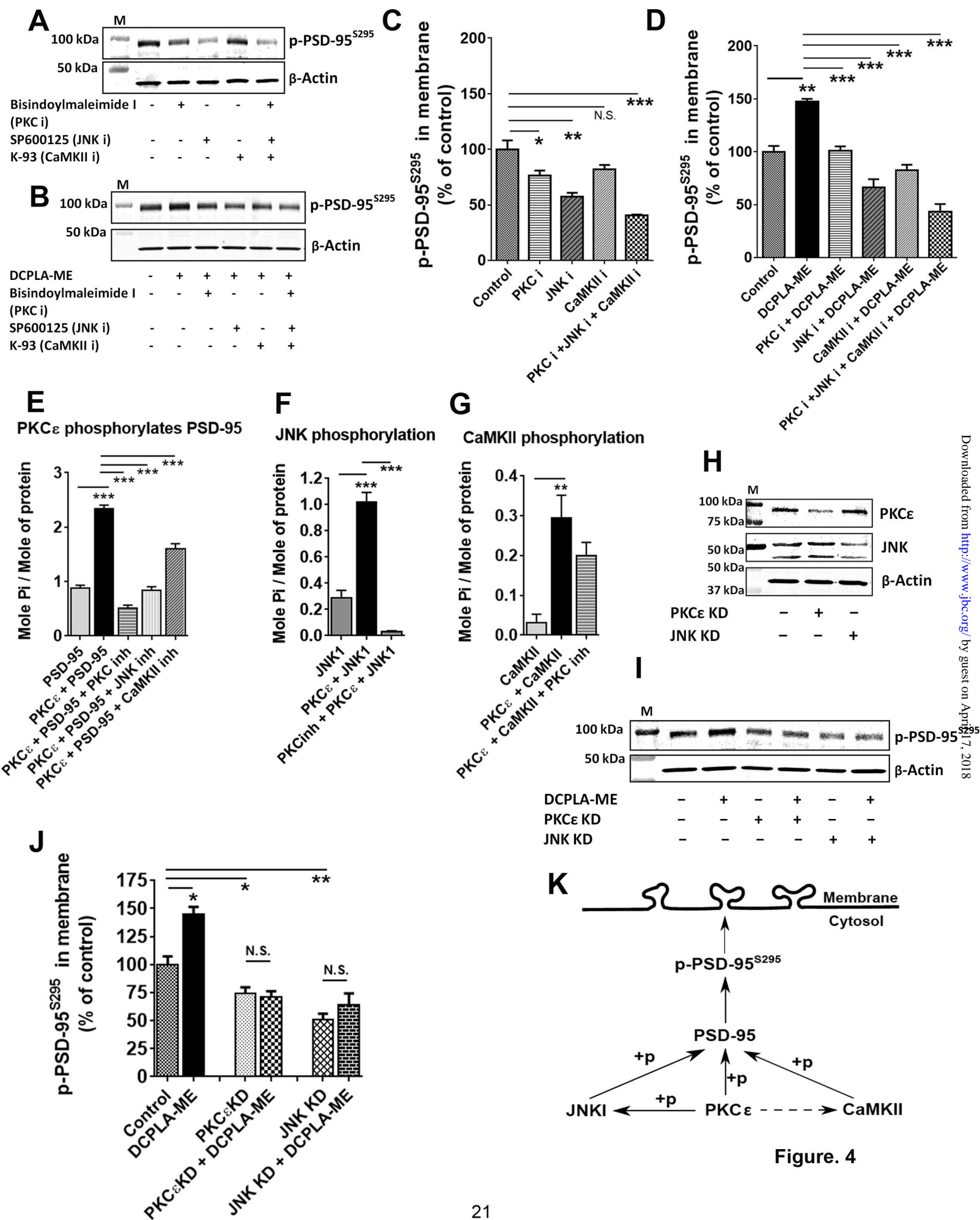
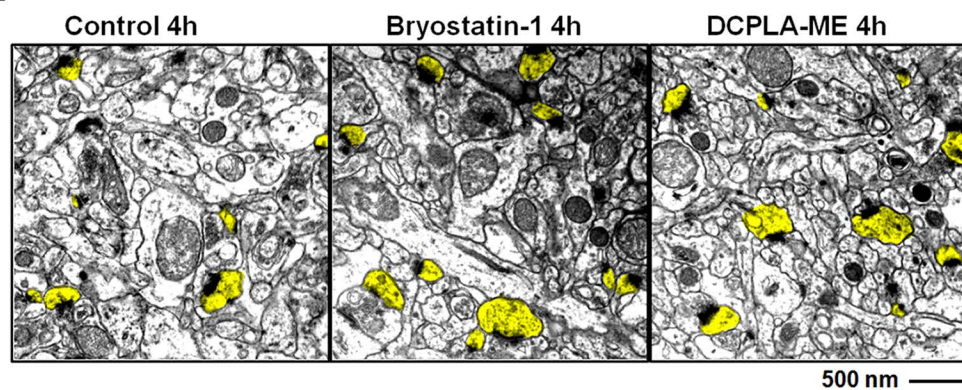
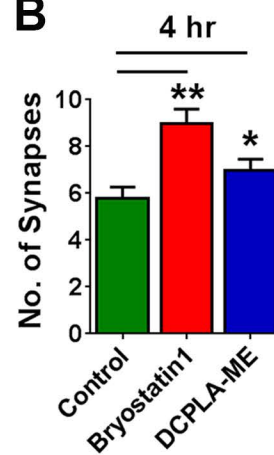
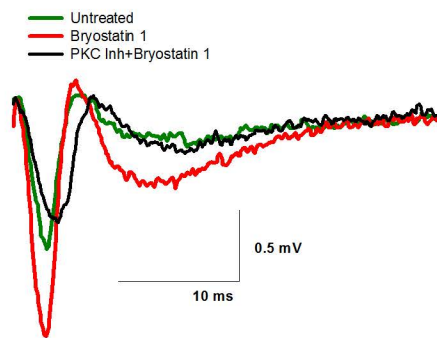


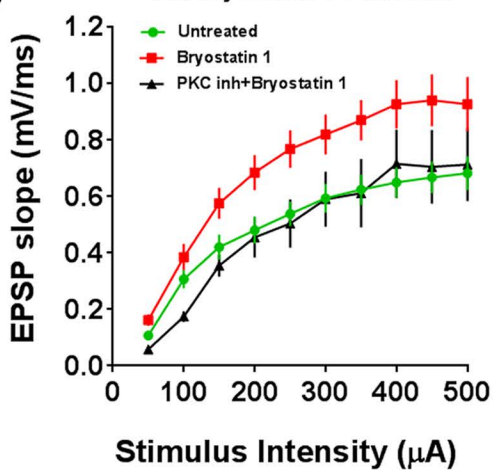
Figure. 4

A**B****C**

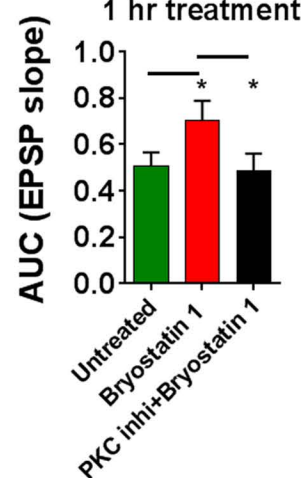
1 hr

**D**

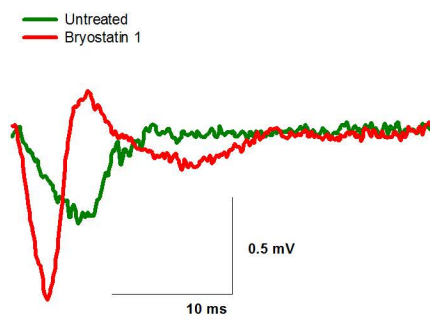
1 hr bryostatin 1 treatment

**E**

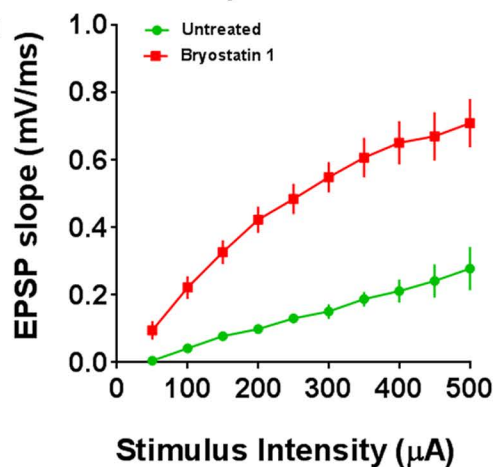
1 hr treatment

**F**

4 hr

**G**

4 hr bryostatin 1 treatment

**H**

4 hr treatment

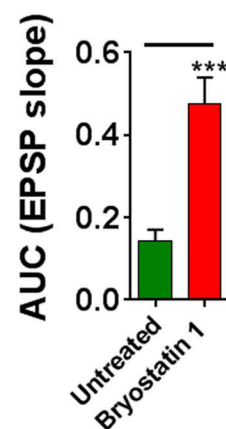


Figure. 5

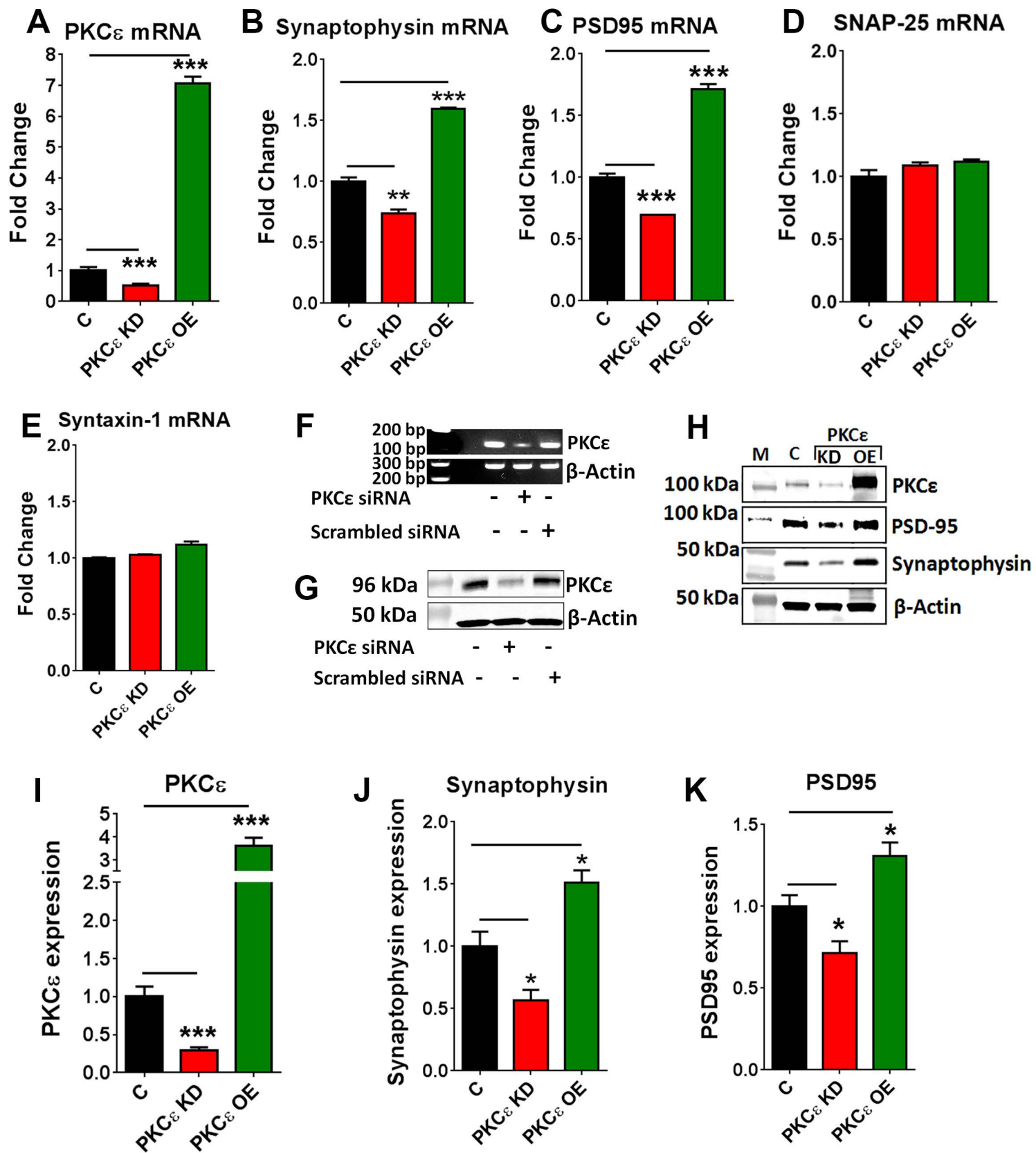
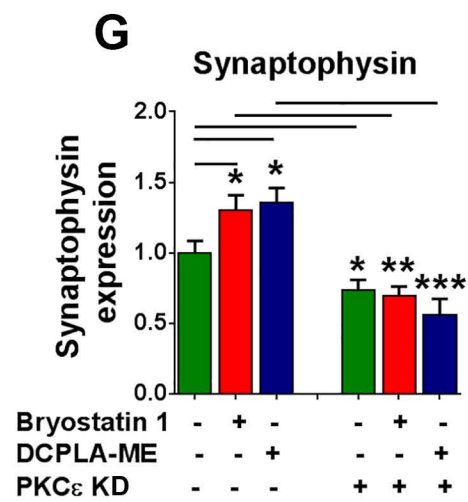
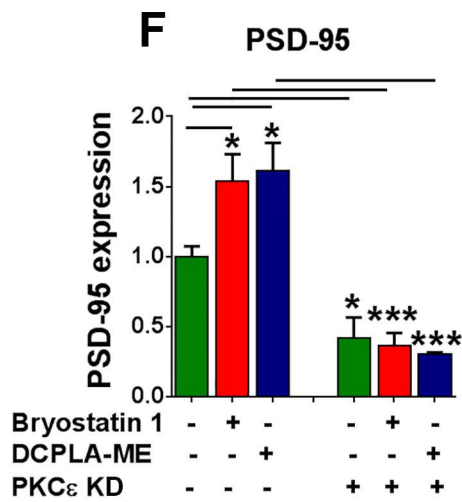
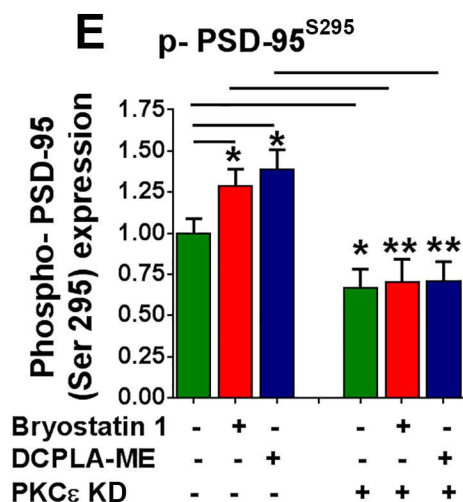
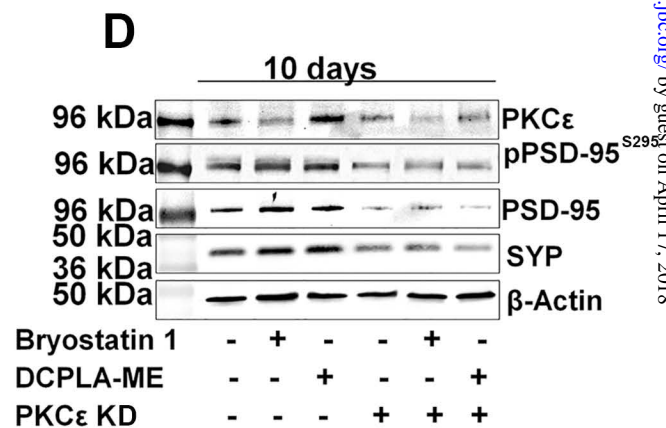
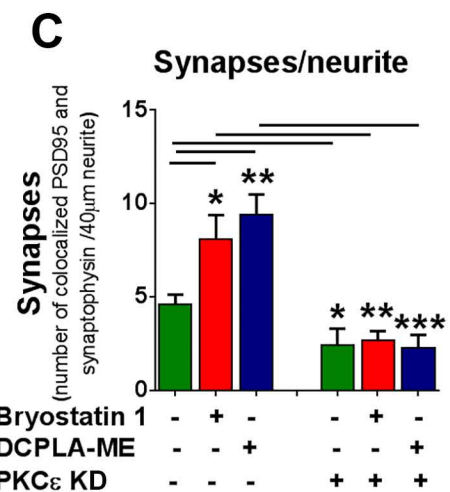
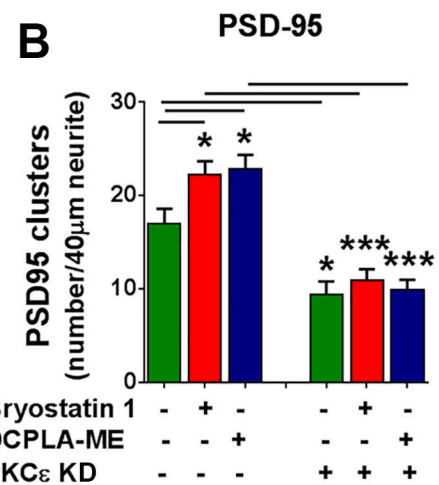
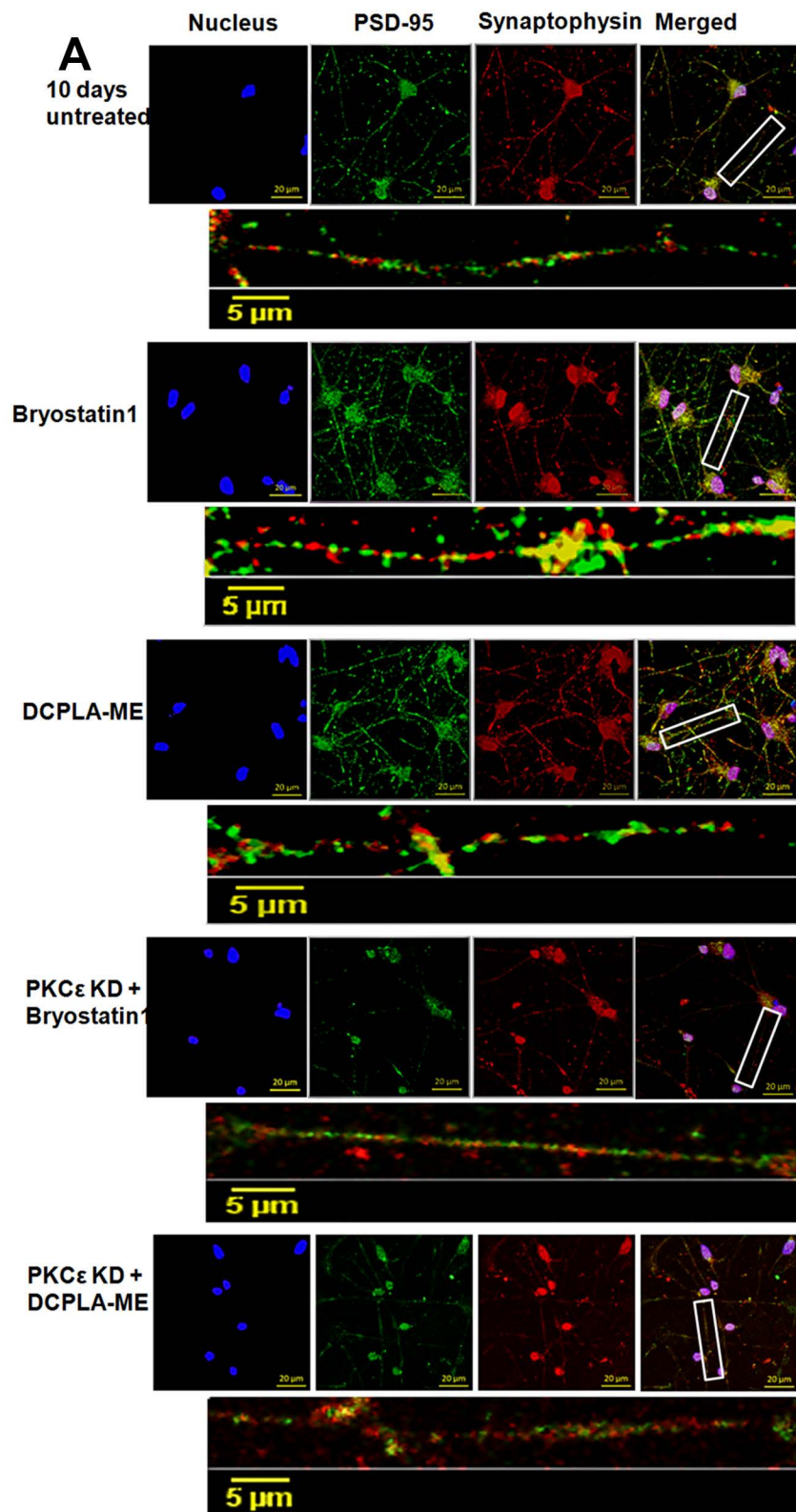


Figure 6



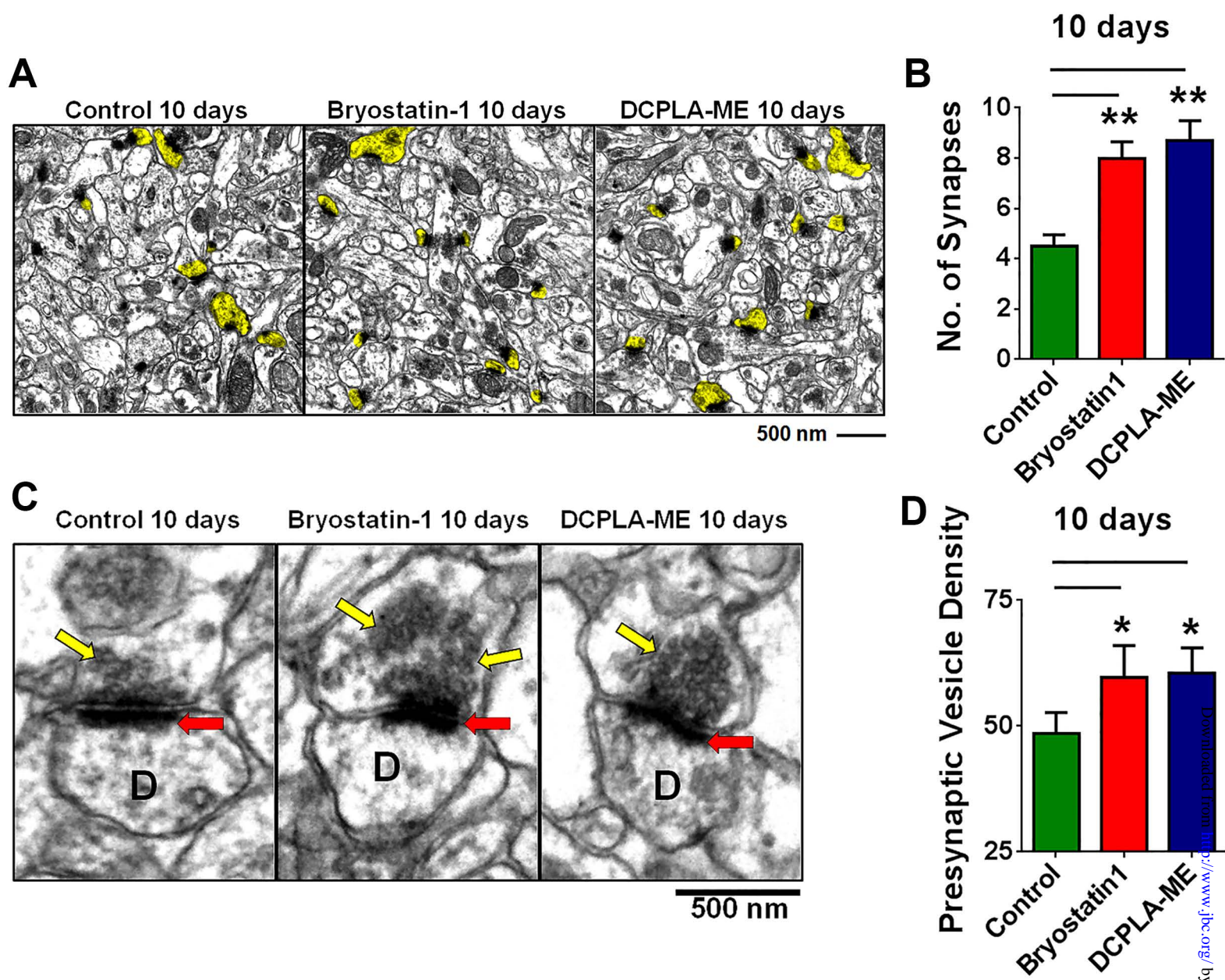


Figure 8

PKC epsilon Promotes Synaptogenesis through Membrane Accumulation of the Postsynaptic Density Protein PSD-95

Abhik Sen, Jarin Hongpaisan, Desheng Wang, Thomas J. Nelson and Daniel L. Alkon

J. Biol. Chem. published online June 21, 2016

Access the most updated version of this article at doi: [10.1074/jbc.M116.730440](https://doi.org/10.1074/jbc.M116.730440)

Alerts:

- [When this article is cited](#)
- [When a correction for this article is posted](#)

[Click here](#) to choose from all of JBC's e-mail alerts

Supplemental material:

<http://www.jbc.org/content/suppl/2016/06/21/M116.730440.DC1>